TEN MICRON OBSERVATIONS OF NEARBY YOUNG STARS

STANIMIR A. METCHEV AND LYNNE A. HILLENBRAND

Division of Physics, Mathematics, and Astronomy, California Institute of Technology, MC 105-24, Pasadena, CA 91125;
metchev@astro.caltech.edu, lah@astro.caltech.edu

AND

MICHAEL R. MEYER

Steward Observatory, University of Arizona, 933 North Cherry Avenue, Tucson, AZ 85721-0065

Received 2003 July 30; accepted 2003 September 16

ABSTRACT

We present new 10 μm photometry of 21 nearby young stars obtained at the Palomar 5 m and at the Keck I 10 m telescopes as part of a program to search for dust in the habitable zone of young stars. Thirteen of the stars are in the F–K spectral type range ("solar analogs"), four have B or A spectral types, and four have spectral type M. We confirm existing *IRAS* 12 μm and ground-based 10 μm photometry for 10 of the stars and present new insight into this spectral regime for the rest. Excess emission at 10 μm is not found in any of the young solar analogs, except for a possible 2.4 σ detection in the G5 V star HD 88638. The G2 V star HD 107146, which does not display a 10 μm excess, is identified as a new Vega-like candidate, based on our 10 μm photospheric detection, combined with previously unidentified 60 and 100 μm *IRAS* excesses. Among the early-type stars, a 10 μm excess is detected only in HD 109573A (HR 4796A), confirming prior observations; among the M dwarfs, excesses are confirmed in AA Tau, CD $-40°8434$, and Hen 3-600A. A previously suggested *N*-band excess in the M3 dwarf CD $-33°7795$ is shown to be consistent with photospheric emission. We calculate infrared to stellar bolometric luminosity ratios for all stars exhibiting mid-infrared excesses and infer the total mass of orbiting dust in the cases of optically thin disks. For a derived median photometric precision of ±0.11 mag, we place an upper limit of $M_{\rm dust} \approx 2 \times 10^{-5}\,M_\oplus$ on the dust mass (assuming a dust temperature of 300 K) around solar analogs not seen in excess at 10 μm. Our calculations for the nearby K1 V star HD 17925 show that it may have the least massive debris disk known outside our solar system ($M_{\rm dust} \gtrsim 7 \times 10^{-6}\,M_\oplus$). Our limited data confirm the expected tendency of decreasing fractional dust excess $f_d = L_{\rm IR}/L_*$ with increasing stellar age. However, we argue that estimates of f_d suffer from a degeneracy between the temperature and the amount of circumstellar dust $M_{\rm dust}$, and we propose a relation of $M_{\rm dust}$ as a function of age instead.

Subject headings: circumstellar matter — dust, extinction — infrared: stars — planetary systems:
protoplanetary disks

On-line material: color figures

1. INTRODUCTION

Since the discovery of far-infrared (FIR) excess emission by the *Infrared Astronomy Satellite* (*IRAS*) toward the main-sequence star Vega (Aumann et al. 1984), nearly 400 other main-sequence stars have been detected with such excesses (Mannings & Barlow 1998; Sylvester & Mannings 2000; Habing et al. 2001; Spangler et al. 2001; Laureijs et al. 2002a; Song et al. 2002 and references therein), interpreted as being due to orbiting dust. Too old to possess remnant primordial dust (which would be cleared by Poynting-Robertson [PR] drag on the timescale of several megayears in the absence of gas), these stars owe their FIR excess to emission by "debris disks," formed by the continual collisional fragmentation of larger bodies (Backman & Paresce 1993 and references therein). Stellar systems exhibiting this phenomenon have been accordingly named "Vega-like." Subsequent higher spatial resolution imaging at millimeter wavelengths of the nearest subsample of Vega-like stars has revealed intricate disklike structures, with gaps and concentrations indicative of ongoing disk clearing by planets (e.g., Holland et al. 1998; Greaves et al. 1998; Jayawardhana et al. 1998; Koerner et al. 1998; Wilner et al. 2002).

While such observations have provided a wealth of information about the outer reaches (>10 AU) of these systems, the "habitable zone" (defined as the region corresponding to the temperature of liquid water) around the majority of them remains at separations unresolvable by direct imaging and can be probed only by interferometry or mid-infrared (MIR) spectroscopy. To first order, however, information about the presence of warm ($\sim$300 K) material around a star can be extracted from its spectral energy distribution (SED) and the presence or absence of an MIR excess above the expected photospheric level.

To date, searches for MIR excesses from both the ground and space have been dominated by upper limits. All Vega-like stars have been identified from *IRAS* and *Infrared Space Observatory* (*ISO*) observations and are therefore limited by their sensitivities ($\sim$0.5 Jy at 12–60 μm for the *IRAS* Point Source Catalog). In a sample of nearly 150 stars in the 1–630 Myr age range, Spangler et al. (2001) find that the vast majority of targets older than $\sim$20 Myr have either no measurable 12 and 25 μm excesses or no detections from *IRAS*. Nevertheless, given a gradually decreasing dust fraction for young stars (Spangler et al. 2001; Habing et al. 1999), more sensitive MIR observations are expected to uncover less massive debris disks around older stars.

Young stars form a particularly suitable set of targets to search for MIR emission from circumstellar disks. They are

likely to be at a transition stage, where the innermost regions of the dust disk have been cleared, whereas, because of an increase of the viscous and dynamical timescale with radius (Hollenbach, Yorke, & Johnstone 2000; Nakagawa, Hayashi, & Nakazawa 1983), cooler material may still be present farther away. No excess is expected at near-infrared (NIR) wavelengths (1–5 μm; $\lesssim$0.1 AU) from these stars, yet longer wavelength excess due to more distant (0.1–10 AU), cooler material could be detectable.

Except for stars within a few tens of parsecs, stellar photospheres are not detected at 12 μm with the small apertures of *IRAS* and *ISO*. However, the recent availability of MIR instrumentation on 5–10 m class ground-based telescopes has made them competitive with *IRAS/ISO* within the atmospheric windows at 10 and 20 μm, with limiting flux densities $\lesssim$20 mJy detectable at 10 μm. In particular, for sufficiently nearby and sufficiently young stars, sensitivity to stellar photospheres is achieved. This implies sensitivity to a small excess above the photosphere and hence to debris disks $\sim10^{-5} M_\oplus$, limited by photometric precision. In addition, the higher angular resolution attainable with large ground-based telescopes allows for unambiguous determination of the origin of the IR flux within the *IRAS/ISO* beam. We can thus discriminate between Vega-like excesses associated with the star and apparent excess flux associated, instead, with a background object in the *IRAS* or *ISO* beam (Aumann & Probst 1991; Lisse et al. 2002), structure in the IR cirrus, or due to detection threshold bias (Song et al. 2002).

In this paper we present 10 μm photometry of 21 nearby stars spanning the $\sim$1–600 Myr age range and thus expected to cover the stages in the transition between a primordial and a debris disk. Age estimates are obtained from the literature and are based on high-resolution spectroscopic measurements of lithium abundances and/or from inferred association with known kinematic groups of stars. Our sample was selected to include nearby ($\lesssim$150 pc) stars, covering a wide range of spectral types (B9–M4), for which the photosphere should be detectable at 10 μm from the ground.

Twelve of our targets have *IRAS* and/or *ISO* detections, eight of which have already been inferred to harbor debris disks. For these objects, our 10 μm data test the existence of possible excess at shorter wavelengths.

2. GROUND-BASED 10 μm PHOTOMETRY

Observations were conducted under marginally photometric conditions at 10.7 μm with the Long Wavelength Spectrograph (LWS; Jones & Puetter 1993) on the Keck I 10 m telescope during two runs (2000 February 20–21 and December 9) and under photometric conditions at 10.3 μm with SpectroCam-10 (SC-10; Hayward et al. 1993) on the Hale 5 m telescope on 2002 January 1 and 3. The 10.7 μm LWS filter has an FWHM of $\approx$1.6 μm,[1] and the 10.3 μm SC-10 filter has a bandwidth of $\sim$1 μm (Hayward, Houck, & Miles 1996,[2] p. 6); thus, they are both longward of the telluric ozone feature at 9.6 μm and of the peak of the potential photospheric silicate emission at 9.7 μm.

Table 1 lists the instrument and epoch of observation for each source.

2.1. *LWS Data*

LWS is a Boeing-made 128^2 pixel Si:As moderate-flux array, mounted at the Forward Cassegrain module on the Keck I telescope, providing diffraction-limited imaging (10$''$ field of view, 0$\farcs$08 pixel^{-1}) and spectroscopic ($R = 100$ and 1400) capabilities in the 3.5–25 μm wavelength range. For the observations presented here we used only the imaging mode

---

[1] See http://www2.keck.hawaii.edu/inst/lws/filters.html.
[2] Available at http://www.astro.caltech.edu/palomar/200inch/spectrocam/scdoc.html.

TABLE 1
OBSERVATIONAL EPOCHS

Star	Other ID	Date (UT)	Instrument	Association
AA Tau.................	IRAS F04318+2422	2000 Feb 21	LWS	Taurus CTTs
DI Tau..................	. . .	2000 Feb 21	LWS	Taurus WTTs
CD −33°7795.......	TWA 5A	2000 Feb 20	LWS	TW Hya WTTs
Hen 3-600A	TWA 3A	2000 Feb 20	LWS	TW Hya CTTs
HD 109573A.........	HR 4796A	2000 Feb 21	LWS	TW Hya
CD −38°6968.......	RX J1109.7−3907	2000 Dec 9	LWS	TW Hya WTTs[a]
HD 147809	HIP 80425	2000 Feb 20	LWS	Upper Sco
HD 145519	SAO 159767	2000 Feb 20	LWS	Upper Sco
HD 102647	HIP 57632	2000 Feb 20	LWS	Field star
HD 17925	HIP 13402	2000 Feb 21	LWS	Field star
CD −40°8434.......	IRAS 14050−4109	2000 Feb 21	LWS	Field WTTs
HD 216803	HIP 113283	2000 Dec 9	LWS	Field star
AP 93	V525 Per	2002 Jan 1	SC-10	α Per
RE J0137+18A	RX J0137.6+1835A	2002 Jan 1	SC-10	Field star
RE J0137+18B......	RX J0137.6+1835B	2002 Jan 1	SC-10	Field star
HD 60737	HIP 37170	2002 Jan 1	SC-10	Field star
HD 70573	SAO 116694	2002 Jan 3	SC-10	Field star
HD 70516	HIP 41184	2002 Jan 3	SC-10	Field star
HD 77407	HIP 44458	2002 Jan 3	SC-10	Field star
HD 88638	HIP 50180	2002 Jan 3	SC-10	Field star
HD 107146	HIP 60074	2002 Jan 3	SC-10	Field star

[a] Candidate TWA member (Sterzik et al. 1999).

of LWS at 10.7 μm. The seeing was poor and variable: 0″3–0″6 at 10 μm (the attainable diffraction limit is 0″22). Data were taken in the standard manner employed for MIR observations, with both chopping and nodding to off-source positions. The resulting images were processed and co-added using the LWSCOADD routine written in IDL by Gregory D. Wirth.[3] No flat-fielding was performed, as this was found to increase the scatter in the photometry. Instead, we attempted to place the stars always in the same place on the array.

Magnitudes were obtained based on measurements of 10 Infrared Telescope Facility (IRTF) N-band standard stars (Tokunaga 1984; Rieke, Lebofsky, & Low 1985). Photometry was performed with the IRAF/PHOT task in apertures of radius 0″96 (12 pixels), with sky background measured in 2″0–3″2 radius (25–40 pixel) annuli. A curve-of-growth correction (-0.12 ± 0.01 mag, based on standard-star measurements) to a 1″92 (24 pixel) aperture was then applied to each star to bring the magnitudes to within $\approx$2% of the infinite aperture value. An atmospheric extinction correction of -0.32 ± 0.07 mag per air mass was derived based on standard-star observations, where we have allowed for $\approx$20% shifts in the night-to-night atmospheric zero points to align the extinction curves from each night. The rms scatter in the photometry of the standards is 0.06 mag for 2000 February 20 and 21 and 0.13 mag for 2000 December 9.

2.2. SC-10 Data

SC-10 is a 128^2 pixel Si:As BIBIB (Back Illuminated Blocked Impurity Band) detector manufactured by Rockwell. For our program we used it in imaging mode (16″ field of view) with a 10.3 μm filter, although the instrument also allows $R = 100$ and 2000 spectroscopy between 5 and 20 μm. The seeing was poor, 0″7 at 10 μm, but relatively stable. Both chopping and nodding were used in the data acquisition, with the chop and the nod throws being of the same magnitude ($\approx$20″). The chip was binned into a 64×64 pixel array with 0″256 pixels, providing nearly Nyquist sampling of the diffraction limit (0″48) of the telescope, and then stored into a three-dimensional image, each slice of which contained a co-added chopped frame. Dark frames were taken for all source exposure times and subtracted from all frames. Flat fields were constructed by median-combining the off-source exposures for each target. This approach of obtaining a flat field was preferred to making a master flat from all exposures during the night because of an unexplained $\sim$4″ shift in the filter vignetting pattern across the field of view over the course of the observations. The rms scatter in the flat fields was $\lesssim$1%.

Final images from SC-10 were obtained by differencing each nodded pair and then averaging the differences. Since source reacquisition during nodding was not perfect, the point-spread function (PSF) of the final image was broader (FWHM $\approx$ 3 pixels = 0″77) than the diffraction limit. Attempts with centroiding the target in each differenced pair before co-adding were not successful because only the standard stars had enough signal-to-noise ratio (S/N) to obtain good centroids. Object magnitudes were measured on the reduced images in 1″5 radius (6 pixel) apertures, using the IRAF/PHOT task. Local sky was estimated as the mode of the pixels in a 3″8–5″1 (15–20 pixel) annulus around each object. An aperture correction (-0.147 ± 0.014 mag, determined

from measurements of standard stars) to a 3″1 (12 pixel) aperture was then applied to bring the estimate of the enclosed flux to within $\approx$2% of its infinite aperture value. In the case of the double source RE J0137+18A/B (1″7 separation) magnitudes were obtained through PSF fitting with DAOPHOT/ALLSTAR (Stetson 1987), using a 3″1 radius PSF fit to the standard star β And, observed immediately beforehand. An air-mass correction of -0.13 ± 0.03 mag per air mass, as determined from observations of the standard stars α Boo and β Gem on 2002 January 3, was applied to all measured magnitudes. The rms scatter in the photometry of the standards is 0.015 mag for 2002 January 1 and 0.007 mag for January 3.

3. SEDS AND PHOTOSPHERIC MODELS

3.1. Optical and Infrared SEDs

SEDs for the observed stars are presented in Figure 1, with our 10 μm photometry plotted as filled circles. $UBVRILMNQ$ measurements were collected from the literature, where available. JHK_s photometry was extracted from the Two Micron All Sky Survey (2MASS) Point Source Catalog for all but the brightest sources (HD 216803, HD 102647, HD 17925, and HD 109573A), the data for which were taken from Aumann & Probst (1991) and Jura et al. (1993). For the $UBVRI$ and $JHKLMNQ$ sets of filters, conversion from magnitudes to flux densities F_λ was performed using the zeroth-magnitude flux densities listed in Allen (1973) and Cohen et al. (1992), respectively. For the objects with 2MASS photometry, the transformation from JHK_s magnitudes to flux densities was based on the calibration by Cohen, Wheaton, & Megeath (2003), outlined in the 2MASS Explanatory Supplement (Cutri et al. 2003,[4] chap. VI.4a). For the N filter we have adopted the same conversion factor for both the 10.3 (SC-10) and 10.7 μm (LWS) filters. Given the difference in central wavelengths of the two N-band filters, the derived zero-magnitude flux densities are expected to be within $\approx$4% of each another.

$IRAS$ fluxes and upper limits were obtained from the $IRAS$ Faint Source Catalog (FSC), or from the Point Source Catalog (PSC) when the FSC did not contain the object (HD 147809, HD 109573A, and the 100 μm data point for CD $-40°$8434). FSC photometry was given preference over the PSC because of its higher S/N and superior sensitivity to faint objects. Reduced ISO data in the 12–60 μm range were available for five of our targets. For HD 17925 and HD 102647 we adopted the color-corrected 25 μm ISO flux densities presented in Laureijs et al. (2002a); the 11.5 and 20 μm data for HD 216803 are from Fajardo-Acosta et al. (1999), and 60 μm measurements for HD 145519 and HD 147809 were taken from M. Meyer et al. (2004, in preparation). The ISO Data Centre lists that additional data were obtained for five of our targets (HD 147809, HD 145519, HD 216803, CD $-40°$8434, and AP 93), none of which were user-reduced, however. For the sources with no available reduced $IRAS$ or ISO data we have adopted nominal $IRAS$ all-sky survey detection limits away from confused regions of the sky: 0.5 Jy at 12, 25, and 60 μm, and 1.5 Jy at 100 μm.

The $IRAS$ and ISO flux densities were color-corrected assuming blackbody emission, following the procedures outlined in the $IRAS$ Explanatory Supplement (Beichman et al. 1988, chap. VI.C.3) and the ISO Handbook (Laureijs et al.

---

[3] Available at http://www2.keck.hawaii.edu/inst/lws/lwscoadd_pro.html.

[4] Available at http://www.ipac.caltech.edu/2mass/releases/allsky/doc/explsup.html.
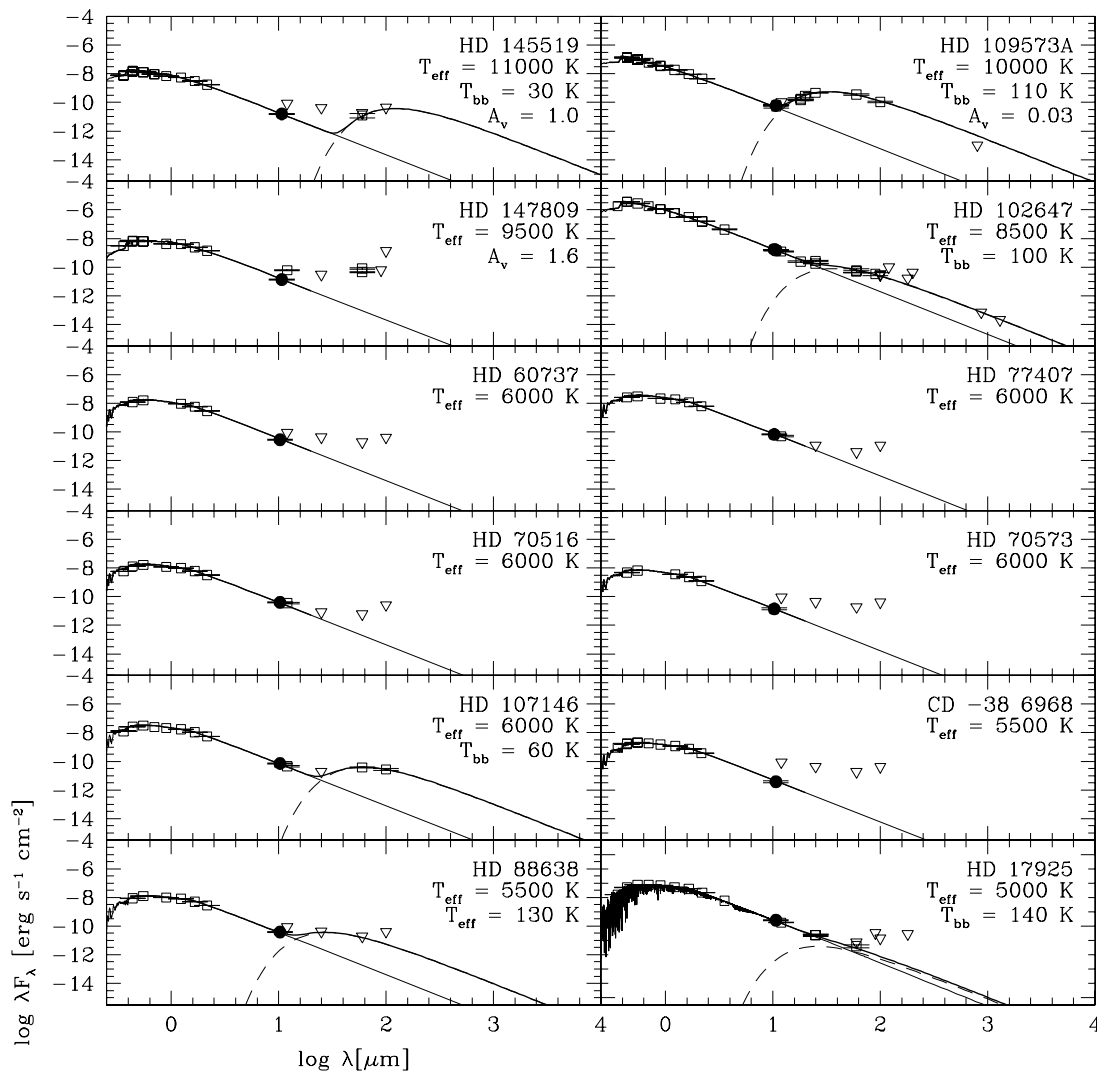
Fig. 1a

Fig. 1.—SEDs of the observed stars. Our 10 μm data are plotted with filled circles, while data from the literature are plotted with open squares (with error bars where available). Upper limits are plotted as downward-pointing triangles. Photospheric models (*thin lines*; photospheric temperatures listed under the object names) are from Kurucz (1979, 1992) and Hauschildt et al. (1999). Dashed lines represent blackbody fits to the observed excess emission. The total flux densities (photosphere plus blackbody) are plotted with thick lines. [*See the electronic edition of the Journal for a color version of this figure.*]

2002b,[5] Appendix C). The adopted color correction factors were chosen depending on the effective temperature $T_{\rm eff}$ of each star (based on spectral types from SIMBAD, unless otherwise noted; Table 2). For *IRAS* they were 1.41–1.45 at 12 μm, 1.39–1.41 at 25 μm, 1.30–1.32 at 60 μm, and 1.09 at 100 μm, where the range of values corresponds to the range of $T_{\rm eff}$ of the stars in our sample.

NIR and MIR photometry for the observed sources from 2MASS (*JHK$_s$*), *IRAS* (12 μm), and our 10 μm observations is summarized in Table 2. The 12 μm color-corrected magnitudes ([12]) were calculated assuming an *IRAS* color-corrected flux of 28.3 Jy for a zeroth-magnitude star (Beichman et al. 1988, chap. VI.C.2a).

3.2. *Photospheric and Dust Models*

The stellar SEDs in Figure 1 were fitted with photospheric models from Kurucz (1979, 1992) and with NextGen models

from Hauschildt, Allard, & Baron (1999). In fitting model photospheres, we have assumed $\log g = 4.5$ and solar metallicity in all models, as is approximately true for main-sequence dwarfs in the solar neighborhood (Drilling & Landolt 2000). The temperatures of the models were chosen to correspond to the spectral types of the stars (Table 2; de Jager & Nieuwenhuijzen 1987). This produced satisfactory (by eye) fits in most cases, except when nonsimultaneous photometry of variable stars in different filters had to be fitted (e.g., AA Tau, AP 93). For RE J0137+18A/B we found that the required photospheric temperature ($T_{\rm eff} \approx 4700$ K for spectral type K3 V) was too high to fit the optical and NIR SED. We obtain better fits using a NextGen 4200 K photosphere for both stars, which can be explained if both components of the binary had subgiant gravities ($\log g \approx 4.0$; de Jager & Nieuwenhuijzen 1987). Given their young age (~1 Myr), AA Tau and DI Tau are also expected to have subgiant gravities. However, the effect on the model photospheres is small compared to that due to the extinction measured toward both stars ($A_V = 1.0$ and 0.76, respectively; Fig. 1b).
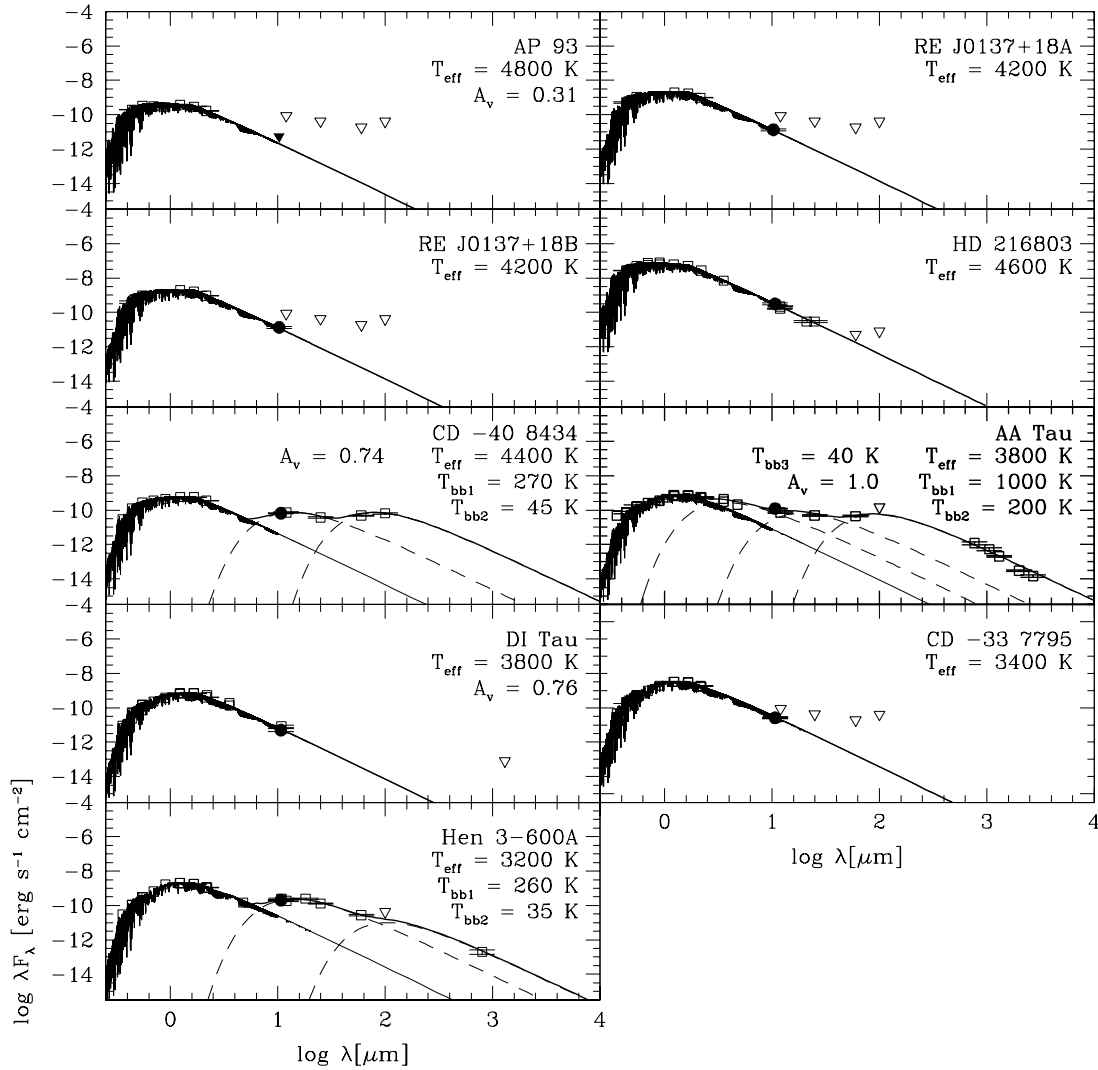
FIG. 1b

The agreement between the two sets of models is satisfactory over the 5000–10,000 K range of temperatures, although at lower temperatures the NextGen models describe the stellar photosphere more closely (Hauschildt et al. 1999). For stars with $T_{eff} \geq 5500$ K, we have chosen to plot Kurucz models, as their lower resolution gives a better visual idea of the integrated flux density of the stellar photosphere at short wavelengths. At wavelengths $\lambda > 20$ μm, for which Kurucz does not predict fluxes, we have linearly extrapolated the model photospheres from the last two (10 and 20 μm) data points. NextGen models (ranging from 10 nm to 10 mm) have been used for all cooler ($T_{eff} \leq 5000$ K) stars.

The model for every star was normalized to each of the measured J, H, and K fluxes (although in Fig. 1 we have shown only the J-band normalizations). The mean predicted photosphere at 10.3 μm (for the SC-10 targets) or at 10.7 μm (for the LWS targets) from the three normalizations was then taken as representative of the photospheric level, and the standard deviation of the mean was taken as the error $\sigma_{N(pred)}$ in the predicted photosphere. The NIR was chosen for normalization because (1) it is close in wavelength to the target band at 10 μm, (2) uniform photometry is available for the majority of our

targets (from 2MASS), and (3) most of our targets were not expected a priori to possess NIR excesses.

We have assumed no circumstellar extinction except in the cases for which an estimate was found in the literature: HD 145519 ($A_V = 1.0$; Krelowski & Strobel 1983), HD 109573A ($A_V = 0.03$; Jura 1991), HD 147809 ($A_V = 1.6$; Eggen 1998), AA Tau ($A_V = 1.0$; Beckwith et al. 1990), AP 93 ($A_V = 0.31$; O'Dell, Hendry, & Collier Cameron 1994), DI Tau ($A_V = 0.76$; Stassun et al. 2001), and CD $-40°8434$ ($A_V = 0.74$; Gregorio-Hetem & Hetem 2002). An extinction law was adopted from Mathis (1990) over the entire SED range (from 0.25 μm to 10 mm).

Table 2 lists the derived 10 μm excesses ΔN for all targets. The quoted error in ΔN is comprised in each case of the photometric error in the measurement of N, and the error $\sigma_{N(pred)}$ in the level of the predicted photosphere. Excluding the stars already known to possess such (HD 109573A, CD $-40°8434$, AA Tau, and Hen 3-600A) and AP 93 (for which we only measure an upper limit to the 10 μm intensity), the mean N-band excess is 0.01 ± 0.03 mag. This is indicative of the accuracy with which the photospheric models are able to predict the broadband 10 μm flux density and demonstrates

TABLE 2

Infrared Photometry and Properties of the Observed Sources

Source	$J-H$ (mag)	$H-K_s$ (mag)	K_s-N (mag)	N (mag)	ΔN (mag)	$K_s-[12]$ (mag)	Spectral Type	Age (Myr)	Parallax (mas)	Notes
HD 145519	0.18 ± 0.04	0.14 ± 0.05	−0.44 ± 0.10	7.04 ± 0.10	−0.10 ± 0.13	<1.29	B9 V	5–8	6.3 ± 0.8	1, 2, 3
HD 109573A........	0.00 ± 0.08	0.00 ± 0.08	0.22 ± 0.12	5.58 ± 0.10	0.29 ± 0.11	<1.25	A0 V	110 ± 5	14.91 ± 0.75	1, 4
HD 147809	0.22 ± 0.06	0.16 ± 0.06	−0.15 ± 0.12	7.21 ± 0.12	−0.11 ± 0.13	1.91 ± 0.11	A1 V	5–8	6.3 ± 0.8	2, 3
HD 102647	0.34 ± 0.02	0.01 ± 0.01	−0.08 ± 0.08	2.06 ± 0.08	−0.03 ± 0.09	0.03 ± 0.06	A3 V	10–300	90.16 ± 0.89	5, 6
CD −38°6968.......	0.29 ± 0.06	0.03 ± 0.05	−0.12 ± 0.19	8.60 ± 0.19	−0.10 ± 0.19	<2.96	G3	<100	7.90 ± 23.80	7
HD 107146	0.27 ± 0.03	0.07 ± 0.03	0.19 ± 0.09	5.35 ± 0.09	0.11 ± 0.09	0.05 ± 0.13	G2 V	50–250	35.07 ± 0.88	8, 9
HD 60737	0.28 ± 0.03	0.06 ± 0.03	−0.11 ± 0.11	6.36 ± 0.11	−0.18 ± 0.11	<0.73	G0	50–250	26.13 ± 1.04	9, 10
HD 70573	0.28 ± 0.04	0.09 ± 0.04	0.05 ± 0.18	7.14 ± 0.18	−0.01 ± 0.18	<1.67	G1/2 V	50–250	11.30 ± 10.70	9, 11
HD 70516	0.28 ± 0.03	0.09 ± 0.02	0.14 ± 0.09	6.00 ± 0.09	0.07 ± 0.09	0.39 ± 0.11	G0	100–300	27.10 ± 2.18	9
HD 77407	0.27 ± 0.03	0.09 ± 0.03	−0.01 ± 0.08	5.45 ± 0.08	−0.08 ± 0.08	0.07 ± 0.11	G0	20–150	33.24 ± 0.91	9, 12
HD 88638	0.27 ± 0.03	0.11 ± 0.03	0.29 ± 0.07	6.04 ± 0.07	0.19 ± 0.08	<0.81	G5	250–1000	26.66 ± 3.09	9
HD 17925	0.39 ± 0.02	0.09 ± 0.01	0.02 ± 0.10	4.00 ± 0.10	0.14 ± 0.11	0.01 ± 0.05	K1 V	50–250	96.33 ± 0.77	5, 8, 9
HD 216803	0.54 ± 0.02	0.11 ± 0.01	0.03 ± 0.14	3.80 ± 0.14	0.06 ± 0.14	0.07 ± 0.06	K4 V	200 ± 100	130.94 ± 0.92	5, 9, 13
CD −40°8434.......	0.73 ± 0.05	0.28 ± 0.05	3.05 ± 0.10	5.49 ± 0.10	3.14 ± 0.12	3.56 ± 0.09	K5	≲10	. . .	14
RE J0137+18A	0.62 ± 0.03	0.14 ± 0.03	0.26 ± 0.14	7.18 ± 0.14	0.15 ± 0.15	<1.92	K3 V	30–55	15.8 ± 5.0	9, 12, 15, 16, 17
RE J0137+18B......	0.61 ± 0.03	0.15 ± 0.03	0.32 ± 0.14	7.23 ± 0.14	0.22 ± 0.15	<1.91	K3 V	30–55	15.8 ± 5.0	9, 12, 15, 16, 17
AP 93	0.50 ± 0.03	0.14 ± 0.03	<1.18	>8.18	<1.1	<3.84	K2	80	5.3	18, 19
AA Tau	0.87 ± 0.05	0.51 ± 0.05	3.23 ± 0.08	4.81 ± 0.07	3.07 ± 0.09	3.58 ± 0.11	M0 V	1	7.1	20
DI Tau	0.72 ± 0.03	0.21 ± 0.03	0.10 ± 0.22	8.29 ± 0.22	−0.08 ± 0.22	. . .	M0.5 V	0.6	7.1	21
CD −33°7795.......	0.68 ± 0.04	0.24 ± 0.04	0.24 ± 0.10	6.50 ± 0.10	−0.11 ± 0.10	<1.23	M3 V	10 ± 5	18 ± 3	4, 22
Hen 3-600A	0.62	0.30	3.04 ± 0.20	4.26 ± 0.19	2.54 ± 0.10	3.48 ± 0.09	M4	10 ± 5	18 ± 3	4, 22, 23, 24

Notes.—(1) *JHK* photometry from Jura et al. 1993. (2) Assumed age for Upper Sco OB association is 5–8 Myr (de Geus et al. 1989). (3) Mean distance for Upper Sco from de Geus et al. 1989; Jones 1971. (4) Assumed TW Hya age is 10 ± 5 Myr. (5) *JHK* photometry from Aumann & Probst 1991. (6) Maximum age estimate from Song et al. 2001; minimum age estimated from the lack of known accretion signature in this star. (7) Age estimate from Sterzik et al. 1999. (8) Age deduced from Li measurement of Wichmann, Schmitt, & Hubrig 2003. (9) Age estimate from comparison of unpublished Li λ6707 equivalent width to open cluster sequence. (10) Spectral type from Houck & Swift 1999. (11) Age deduced from Li measurement reported in Jeffries 1995. (12) Age estimate from Montes et al. 2001. (13) Age estimate from Barrado y Navascuès 1998. (14) Age estimate based on Li measurement and spectral type estimate in Gregorio-Hetem & Hetem 2002. (15) The binary is unresolved in 2MASS; *JHK_s* photometry from adaptive optics observations by S. A. Metchev & L. A. Hillenbrand 2004, in preparation. (16) Spectral type from Jeffries 1995. (17) Distance estimate from Montes et al. 2001; consistent with being a nearby member of the Cas-Tau OB association (E. Mamajek 2003, private communication). (18) A 3 σ upper limit at 10 μm. (19) Spectral type deduced from effective temperature listed in Randich et al. 1998. (20) Age estimate from Beckwith et al. 1990. (21) Age estimate from Meyer et al. 1997. (22) Distance obtained as the average of the distances to the four TWA members with *Hipparcos* astrometry: TW Hya, HR 4796A, HD 98800, and TWA 9 (56, 67, 47, and 50 pc, respectively). (23) The binary is unresolved in 2MASS; *JHK* photometry from Webb et al. 1999. (24) Spectral type from Torres et al. 2000.

that the models do not systematically overestimate or underestimate the stellar photosphere at N band.

Excess IR emission, whenever apparent in the SED of a star, was fitted by a single blackbody curve, as would be expected from a narrow ring of dust at a fixed distance from the star. The temperature of the blackbody curve (T_{bb}) is identified for each case in Figure 1. The fits were performed by eye, and experimentation with a range of values for T_{bb} showed that the determined temperatures were generally accurate to $\pm10\%$. For CD $-40°8434$, AA Tau, and Hen 3-600A, single-temperature blackbody emission could not account for the excess at wavelengths greater than 60 μm, and for these stars we have allowed for additional, cooler blackbodies (T_{bb1}, T_{bb2}, etc). Although a disk model would be more appropriate for fitting the observed excesses, our simplistic treatment allows us to estimate color correction factors for the *IRAS* and *ISO* data (which were then reapplied instead of the ones based on the stellar T_{eff}) and to obtain approximate measurements of the dust luminosity fraction in each case.

HD 17925 and HD 145519, with significant excesses only at 60 μm, are the only stars for which we have not applied any color corrections at wavelengths $\geq$60 μm. The large uncertainty in the blackbody temperatures (30–250 K for HD 17925, 30–140 K for HD 145519) that fit the FIR excesses and upper limits for these stars correspond to a range of values for the color correction (0.91–1.19 for *IRAS* at 60 μm for HD 17925, 0.93–1.08 for HD 145519). Thus, the plotted (Fig. 1) *IRAS* and *ISO* flux densities and upper limits for these stars at wavelengths $\geq$60 μm correspond to flat spectrum sources ($F_\nu \propto \nu^{-1}$), as is the default calibration for *IRAS* and *ISO*.

4. RESULTS

4.1. *Stars with Confirmed Excesses*

Ten of our sample stars have been previously reported to possess MIR or FIR dust excesses: HD 145519, HD 109573A (HR 4796A), HD 147809, HD 102647 (β Leo), HD 17925, AA Tau, DI Tau, CD $-40°8434$, Hen 3-600A, and CD $-33°7795$. Three among these (HD 145519, HD102647, and HD 17925) have known 60 μm dust emission from *ISO* and/or *IRAS* (Backman et al. 1997; Laureijs et al. 2002a; Habing et al. 2001) but do not exhibit significant excesses at 10 μm, in agreement with previous measurements. A fourth, DI Tau, previously suspected of harboring warm circumstellar dust on the basis of 12 μm *IRAS* data (Skrutskie et al. 1990), has subsequently been shown not to possess an excess at 10 μm (Meyer et al. 1997), and all of the excess *IRAS* flux can be attributed to the neighboring (15″1) DH Tau. Our photometry of DI Tau is consistent with that of Meyer et al. (1997) and with the lack of circumstellar dust.

Of the remaining six stars that have been reported previously to possess excesses at 10 or 12 μm, we confirm such in four of them: HD 109573A (Jura et al. 1998), AA Tau (Strom et al. 1989), CD $-40°8434$ (Gregorio-Hetem et al. 1992), and Hen 3-600A (Jayawardhana et al. 1999a). Our N-band data for these four objects agree very well with the previously published 10 μm photometry, as well as with the color-corrected *IRAS* 12 μm flux densities, and we will not discuss their photometry further.

4.2. *Stars with Unconfirmed Excesses*

There are two stars (CD $-33°7795$ and HD 147809) for which our nondetection of excess at 10 μm is in disagreement with previous data and interpretations.

4.2.1. *CD $-33°7795$*

Jayawardhana et al. (1999b) report a possible 2.6 σ detection of a 10 μm excess in the M3 V star CD $-33°7795$. Their claim is based on a measured flux density of 96 $\pm$ 9 mJy and an estimated photospheric level of 70 $\pm$ 5 mJy at 10.8 μm, assuming $K-N = 0.0$. Our 10.7 μm flux density (93 $\pm$ 8 mJy) is consistent with theirs and with the level of photospheric emission (100 $\pm$ 5 mJy) found from the NextGen model. The predicted $K-N$ color by the NextGen model is 0.27, which agrees with the measured $K_s-N = 0.24 \pm 0.04$ for this star. For comparison, Kenyon & Hartmann (1995) list $K-[12] = 0.49$ mag for M3 V main-sequence stars, which is expected to be comparable to their $K-N$ color. There is thus no indication of excess emission at 10 μm in this object. Jayawardhana et al. (1999b) acknowledge that if $K-N \sim 0.3$, their measurement would be consistent with being photospheric.

4.2.2. *HD 147809*

Our 10.7 μm measurement of 46 $\pm$ 6 mJy for this star, while consistent with being photospheric, is a factor of 5 fainter than the *IRAS* flux density of 243 $\pm$ 24 mJy at 12 μm. HD 147809 is detected at 12 and 60 μm (S/N $\approx$ 5 in both bands) but is listed only in the PSC, despite being fainter than the nominal PSC sensitivity at 12μm ($\sim$0.5 Jy) and brighter than the sensitivity limit of the FSC ($\sim$0.2 Jy). However, the *IRAS* Faint Source Catalog Rejects (FSCR) lists a 12 μm source (IRAS Z16219$-$2514) within 5″ of HD 147809 (associated with IRAS 16219$-$2514), a separation equal to a fifth of the angular resolution of *IRAS* at 12 μm. The reason for rejection (and inclusion in the FSCR) is that IRAS Z16219$-$2514 is detected only in one band (12 μm) in the FSC, with S/N of 3–6 (Moshir et al. 1992; actual S/N = 5.9). The FSCR also lists one nearby 100 μm–only cirrus extraction ("cirrus" flag 1), which may have possibly affected the PSC 60 μm measurement. The possibility that the 60 and 12 μm PSC detections are associated with IR cirrus is explored below.

HD 147809 is a member of the Upper Scorpius OB complex in the ρ Oph region, which is associated with highly variable background emission in the MIR and FIR (Ryter, Puget, & Pèrault 1987), as seen in the *IRAS* maps of this area. Backman et al. (1997) observe the star with *ISO* at 60 and 90 μm with a detection only at 60 μm: 0.91 $\pm$ 0.07 Jy (S/N = 13), 4 σ fainter than the 1.64 $\pm$ 0.18 Jy flux listed in the *IRAS* PSC at this wavelength. This is possible if the peak of the 60 μm source was in the central (45″ × 45″) pixel of the 3 × 3 PHT-C100 *ISO* array and if the emission extended over the eight border pixels, which were used to estimate local background. *IRAS* photometry, on the other hand, does not involve local background subtraction (each survey scan is initiated and terminated with a flash of the internal reference source to monitor responsivity of the system; Beichman et al. 1988, chap. VI.B.1) and thus measures the total flux in the *IRAS* beam (60″ at 60 μm; Beichman et al. 1988, chap. II.C.3). The lower *ISO* flux density is therefore indicative of the extended nature (over several C100 pixels: $\gtrsim$50″) of the 60 μm emission. At the distance of the Upper Sco OB association ($\sim$160 pc; de Geus, de Zeeuw, & Lub 1989; Jones 1971), the physical size of the structure would be $\sim$10, 000 AU. While it is possible that HD 147809 possesses a dust disk of such size, the corresponding dust temperature (10–30 K) is inconsistent with the 90 μm *ISO* upper limit

(read off from the default *ISO* poststamp measurement representation[6]).

If the 12 μm excess in HD 147809 were associated with orbiting circumstellar material around the star, the ratio of the PSC 12 and 25 μm (upper limit) flux densities $S_\nu(12\ \mu m)/S_\nu$ (25 μm) $\geq 0.95 \pm 0.09$ would require a blackbody temperature $T_{bb} \geq 154$ K (3 σ lower limit), whereas the measured $S_{bb}(10.7\ \mu m)/S_\nu(12\ \mu m) = 0.19 \pm 0.03$ requires $T_{bb} = 65 \pm 5$ K. Therefore, the 12 μm emission either arises outside our 1″ radius LWS aperture or is extended over at least several arcseconds, so that its intensity in the LWS aperture is comparable to that in the background annulus (2″0–3″2). An $S_\nu(12\mu m)/S_\nu$ (25 μm) ratio greater than unity may be indicative of nonthermal emission from aromatic infrared lines in the 12 μm band, as previously suggested in association with interstellar cirrus in ρ Oph (Meyer, Wilking, & Zinnecker 1993; Ryter et al. 1987).

Summarizing the evidence presented above, we conclude that the 12 and 60 μm excesses in the SED of HD 147809 are not associated with the star but are likely due to interstellar cirrus.

4.3. *New Excess Detections*

We find previously unknown IR excesses in three of our target stars. HD 88638 is the only one for which we present new evidence for possible excess emission at 10 μm. HD 107146 is an overlooked Vega-like star from *IRAS*, and HD 70516 has a 29″ distant companion probably responsible for the 12 μm *IRAS* excess.

4.3.1. *HD 88638*

The flux measured from this star at 10.3 μm is 2.4 σ ($\Delta N = 0.19 \pm 0.08$ mag) above the 5500 K, solar metallicity and gravity (log $g = 4.5$) Kurucz photosphere. Given the Hauschildt et al. (1999) claim that the NextGen models better approximate the stellar photosphere at effective temperatures $\lesssim 5500$ K and the spectroscopically determined $T_{eff} = 5360$ K for this star (Strassmeier et al. 2000), we also fitted a 5400 K solar gravity and metallicity NextGen model to the SED. The observed excess is 2.3 σ over the NextGen model: $\Delta N = 0.18 \pm 0.08$ mag; i.e., the excess is nearly model independent.

There is no measurement of the gravity or metallicity of HD 88638 in the literature. Given its *Hipparcos* distance (38 ± 4 pc) and magnitude ($V = 8.02$) and a bolometric correction of -0.165 (Flower 1996), the star should have a luminosity of $L_* = 0.83 \pm 0.15\ L_\odot$ and a radius of $R_* = 1.07 \pm 0.10\ R_\odot$. Assuming $\sim 1\ M_\odot$ for a G5 star of this luminosity, its gravity is log $g = 4.4$, i.e., nearly solar. Alternatively, if subsolar metallicity were causing the higher 10 μm flux, it would have to be ≤ -2.0 dex for the Kurucz model photosphere to fall within 1 σ of our N-band measurement. Such low metallicity would imply that HD 88638 is a halo (Population II) star, whereas its space velocity $(U, V, W) = -(62.6,\ 8.5,\ -1.3)$ (Strassmeier et al. 2000) places its orbit in the plane of the Galactic disk (Population I). Gravity and metallicity effects are thus unlikely to be the cause for the observed excess.

Interstellar extinction of order $A_V \approx 0.1$ could contribute to the abnormal MIR emission. However, HD 88638 is well out of the Galactic plane ($b = +53°46'$), and at 38 pc from the Sun extinction along the line of sight is expected to be negligible.

Moreover, reddened photospheric models normalized to the NIR tend to underestimate the optical flux by ~ 0.2 mag. Hence, extinction is not the probable cause.

The blackbody temperature range that accommodates the excess, the *IRAS* upper limits, and the NIR data is 130–1500 K. This does not exclude a substellar companion of spectral type L6 or later ($T_{eff} \leq 1500$ K). For an L6 dwarf $M_K \gtrsim 11.4$, and assuming $K - N \approx K - L' \gtrsim 1.3$ (Leggett et al. 2002), at the distance of the primary (distance modulus 1.4 mag) the potential companion would have $N \gtrsim 11.5$. The 10 μm excess that this would produce in HD 88638 ($N = 6.04$; Table 2) is $\Delta N \lesssim 0.01$, far too faint to account for what is observed.

Therefore, if real, the 2.4 σ N-band excess is most likely due to orbiting debris. However, from a statistical point of view, a 2.4 σ positive deviation should occur in 0.82% of all observations, if the errors are Gaussian. Given 21 observed sources, a random 2.4 σ excess will occur in 16% of such sets. There is a hence nonnegligible probability that the observed 10.3 μm excess is random.

Because of the marginality of our detection and the large range of possible blackbody temperatures, we have not reapplied the corresponding color correction factors to the *IRAS* upper limits. These would range from 0.90 to 1.36 at 25 μm and from 1.08 to 1.29 at 60 μm (the ones applied based on a 5500 K stellar SED are 1.40 and 1.32, respectively) and will have the effect of allowing a ~ 10 K cooler blackbody fit, i.e., 120 K.

4.3.2. *HD 107146*

Although we do not detect above-photospheric emission at 10 μm from this source, we choose to discuss it here because it has not been previously identified as a Vega-like star, despite 60 and 100 μm excesses measured by *IRAS*. Because its 12 μm *IRAS* flux is consistent with being photospheric, and because of a nondetection at 25 μm, it would have been omitted in most previous searches concentrating on the 12 and 25 μm *IRAS* bands. However, this object has also been missed in the Stencel & Backman (1991) survey for IR excess emission from *IRAS* 12 μm point sources at high Galactic latitude ($|b| > 25°$). This survey selected stars with 12 μm *IRAS* detections from the PSC that were also detected in at least one more *IRAS* band and that had positional association with an SAO star. It was apparently tailored to discover excess IR emission in sources like HD 107146 (SAO 100038, $b = 77.04$), detected in the 12 μm, and in the 60 μm bands in the PSC. However, the low signal-to-noise ratios of these detections, S/N = 3.9 and 6.9, respectively, provide a clue as to why the star may have been overlooked. No *ISO* data exist for this source.

The detection of an excess in this star is not false, as has been suggested for other reported candidate Vega-like stars with low-S/N excess in a single *IRAS* band. The misidentification in those cases is explained as a likely result of detection threshold bias (Song et al. 2002). In the case of HD 107146, however, the FSC (which contains higher S/N measurements for objects fainter than the PSC completeness limits) lists detections of the star in three, rather than two, bands. The higher significance of the detection at 60 μm (S/N = 20) and a 100 μm (S/N = 6) detection make it highly improbable that the excess is due to an upward noise fluctuation. Moreover, our ground-based measurement is consistent with the listed *IRAS* 12 μm flux density and with being photospheric, thus excluding the possibility that the *IRAS* flux comes from an unassociated background object in the *IRAS* aperture.

---

[6] Available at the ESA *ISO* Web site http://www.iso.vilspa.esa.es/ida/index.html.

The IR excess in this star can be fitted by a 60 ± 10 K blackbody. See Williams et al. (2003) for a further discussion of this source, including recent submillimeter observations.

4.3.3. *HD 70516*

The 12 μm *IRAS* detection of this star is listed with a 10 σ significance in the FSC and is 4.1 σ above the NextGen photosphere ($\Delta[12] = 0.45 \pm 0.11$), whereas our 10.3 μm measurement is photospheric ($\Delta N = 0.07 \pm 0.09$). HD 70516 (HIP 41184; G0) is listed as a proper motion binary in the *Hipparcos* catalog, with a $\Delta V = 1.5$ K0 companion (HIP 41181) 29″ away. The separation between the two components matches the resolution of *IRAS* at 12 μm ($\sim$0.5′; Beichman et al. 1988, chap. I.A.1), and it is therefore likely that light from both components contributes to the measured 12 μm flux density. Given V magnitudes of 7.7 and 9.2 for the two stars and expected $V-[12]$ colors of 1.5 and 2.0, respectively (Waters, Cotè, & Aumann 1987), the combined 12 μm magnitude is 5.85, corresponding to $\Delta[12] = 0.35$. Although a significant fraction of the companion's light will fall outside the *IRAS* beam at 12 μm, its vicinity and brightness are marginally consistent with the observed 12 μm excess, making a debris disk interpretation less likely.

The binary is not detected at longer wavelengths with *IRAS* because its expected combined flux density is below the quoted sensitivity limits.

4.4. *Null Excess Detections*

Six of the remaining eight stars do not have 12 μm measurements from *IRAS*: RE J0137+18A/B, HD 60737, HD 70573, CD $-38°6968$, and AP 93. The first five all have 10 μm fluxes consistent with being photospheric. AP 93 (observed with the Palomar 5 m telescope) was not detected at 10 μm. The 3 σ upper limit of 18.8 mJy for this source is

11.0 mJy above the model atmosphere, and we can thus exclude any excess emission at this level.

HD 77407 and HD 216803 have 12 μm measurements from *IRAS*. Our 10 μm photometry for them is consistent with the *IRAS* data, and the models show that the 10–12 μm emission is at the expected photospheric level.

5. DUST PROPERTIES OF STARS WITH EXCESSES

5.1. *Fractional Dust Luminosity f_d*

Table 3 lists the observed dust luminosity fraction $f_d = L_{\mathrm{IR}}/L_*$ for all stars with inferred disks (marked with "Yes" in the last column). These were obtained based on the fitted blackbody curves to the IR excesses. HD 88638 and HD 17925 allow a range of temperatures in the blackbody fits, and for them we have listed a range of values for f_d, with hotter blackbodies generally producing higher fractional luminosities. The measured values for f_d correspond well to the ones found in the literature ($F_{d(\mathrm{Lit})}$; see the last column of Table 3 for references). We are therefore confident that our blackbody fits to the excess IR emission have not introduced significant systematic errors in the estimate of f_d, with respect to estimates based on more elaborate dust and/or debris disk models (e.g., as in Chiang et al. 2001; Li & Lunine 2003).

For the sources without excess emission at 10 μm we estimate $f_d \lesssim 10^{-3}$, approximately corresponding to the 3 σ upper limit on the dust excess that would be produced by a hypothesized 300 K debris ring around a G5 star, assuming our median uncertainty of 0.11 mag in the measured excess ΔN. This is appropriate, since most of the stars that we do not detect in excess are G and K dwarfs. DI Tau is the only M dwarf without a detected excess, and given its later spectral type, the upper limit on f_d is somewhat higher, $f_d \leq 3 \times 10^{-3}$, whereas for HD 147809, the only early-type star (A1 V) not

TABLE 3
Fractional Disk Excesses

Star	Age (Myr)	T_{dust} (K)	f_d	$f_{d(\mathrm{Lit})}$	Reference	Excess?
HD 145519	5–8	30–140	$(2.7–8.0) \times 10^{-4}$	...	1	Yes
HD 109573A.........	10 ± 5	110 ± 10	6.1×10^{-3}	$(5–10) \times 10^{-3}$	2, 3	Yes
HD 147809	5–8	$(300)^{\mathrm{a}}$	$<5 \times 10^{-4}$	...		No
HD 102647	10–300	100 ± 10	2.0×10^{-5}	$(1.2–1.9) \times 10^{-5}$	4, 5	Yes
CD $-38°6968$.......	< 100 (300)	$< 10^{-3}$	...	...		No
HD 107146	50–250	60 ± 10	1.5×10^{-3}	...		Yes
HD 60737	50–250	(300)	$< 10^{-3}$	...		No
HD 70573	50–250	(300)	$< 10^{-3}$	...		No
HD 70516	100–300	(300)	$< 10^{-3}$	...		No
HD 77407	20–150	(300)	$< 10^{-3}$	...		No
HD 88638	250–1000	130–1500	1×10^{-4} to 6×10^{-2}	...		Yes?
HD 17925	50–250	30–250	4×10^{-6} to 3×10^{-4}	1.3×10^{-4}	6	Yes
HD 216803	200 ± 100	(300)	$<5 \times 10^{-4}$	...		No
CD $-40°8434$.......	$\lesssim 10$	$270 \pm 20, 45 \pm 5$	0.24	0.34	7	Yes
RE J0137+18A	30–55	(300)	$< 10^{-3}$	...		No
RE J0137+18B......	30–55	(300)	$< 10^{-3}$	...		No
AP 93	80	(300)	$<7 \times 10^{-3}$	...		No
AA Tau.................	1	$1000 \pm 100, 190 \pm 10, 40 \pm 5$	0.51	0.31	8, 9	Yes
DI Tau..................	0.6	(300)	$<3 \times 10^{-3}$	...		No
CD $-33°7795$.......	10 ± 5	(300)	$< 10^{-3}$	...		No
Hen 3-600A	10 ± 5	$260 \pm 10, 30 \pm 10$	0.16	0.21	3	Yes

[a] For the stars without detected excesses, the listed upper limits of f_d are for assumed 300 K debris disks.

References.—(1) Backman et al. 1997; M. Meyer et al. 2004, in preparation; (2) Jura 1991; (3) Weinberger et al. 2002; (4) Jayawardhana et al. 2001; (5) Spangler et al. 2001; (6) Habing et al. 2001; (7) Gregorio-Hetem & Hetem 2002; (8) Beckwith et al. 1990; (9) Chiang et al. 2001.

seen in excess), $f_d \leq 5 \times 10^{-4}$. For HD 216803, for which the SED is further constrained by the 12 and 25 μm *IRAS* photospheric detections, this upper limit is also $f_d \lesssim 5 \times 10^{-4}$, whereas for AP 93, for which we only have an *N*-band upper limit, $f_d \lesssim 7 \times 10^{-3}$.

5.2. *Dust Disk Parameters*

In estimating the mass of the observed circumstellar dust disks, we have followed the formalism and the steps outlined in Chen & Jura (2001):

$$a \geq a_{\min} = \frac{3L_* Q_{\mathrm{pr}}}{16\pi G M_* c \rho_s}, \tag{1}$$

$$n(a)da = n_0 a^{-p}\, da, \tag{2}$$

$$M_{\mathrm{dust}} \geq \frac{16\pi}{3} f_d \rho_s D^2 \langle a \rangle, \tag{3}$$

$$t_{\mathrm{PR}} = \frac{4\pi \langle a \rangle \rho_s}{3} \frac{c^2 D^2}{L_*}, \tag{4}$$

$$M_{\mathrm{PB}} \geq \frac{M_{\mathrm{dust}}}{t_{\mathrm{PR}}} t_{\mathrm{age}}. \tag{5}$$

Equation (1) gives the minimum particle size $a_{\min}$ that is not blown out by radiation pressure (Artymowicz 1988); L_* and M_* are the stellar luminosity and mass, Q_{pr} is the radiation pressure coupling coefficient, and $\rho_s = 2.5$ g cm^{-3} is the mean density of a dust grain (as assumed in Chen & Jura 2001). Equation (2) represents the assumption that the particle size distribution $n(a)da$ results from equilibrium between production and destruction of objects through collisions (Greenberg & Nolan 1989), where we have assumed $p = 3.5$ (Binzel, Hanner, & Steel 2000). If we weight by the number of particles, the equation can be integrated to obtain an average particle size $\langle a \rangle = 5/3\, a_{\min}$. The inferred dust mass M_{dust} around the star is found from equation (3), where we have assumed that the dust is distributed in a thin shell at a distance D from the star (Jura et al. 1995). If the grains are larger than $\langle a \rangle$, or if colder dust is present ($\lesssim 30$ K; undetectable by *IRAS/ISO*), our estimate of M_{dust} is a lower bound. The Poynting-Robertson lifetime t_{PR} of circumstellar grains is given by equation (4) (Burns, Lamy, & Soter 1979). Since this timescale is generally shorter than the ages (t_{age}) of the stars in our sample (Tables 2 and 3), collisions between larger bodies are required to replenish the grains

destroyed by PR drag. The mass M_{PB} of the parent bodies is given by equation (5).

Stellar parameters (radius R_*, mass M_*, and bolometric luminosity L_*) for stars of spectral type K1 and earlier were estimated using the Allende Prieto & Lambert (1999) database of fundamental parameters of nearby stars, given T_{eff} (based on spectral type) and assuming $\log g = 4.5$. For the cooler ($T_{\mathrm{eff}} < 5000$ K) stars these values were taken from the literature, or, in the case of Hen 3-600A, L_* and R_* were estimated using the star's distance, its visual magnitude (assuming $A_V = 0.0$), and bolometric correction from Flower (1996). Table 4 lists the parameters adopted for each star.

The radiation pressure coupling coefficient Q_{pr}, which enters in the grain size calculation (eq. [1]), was assumed to be ≈ 1, since it deviates from unity only for grains smaller than $\lambda_p/2\pi$ (Burns et al. 1979), where λ_p is the wavelength of peak emission from the host star. For the coolest K dwarf in our sample (RE J0137+18A/B, assumed $T_{\mathrm{eff}} = 4200$ K) $\lambda_p/2\pi = 0.1$ μm, which is comparable to the blowout size for this star. Our assumption that $Q_{\mathrm{pr}} \approx 1$ is therefore valid for K3 and earlier type stars.

In deriving the distance D of the dust shell from the star, we have expanded the discussion in Chen & Jura (2001) by adding a differentiation between grains with blackbody (BB; perfect emitters and absorbers), graybody (GB; imperfect emitters, perfect absorbers), and interstellar medium (ISM; imperfect emitters and absorbers) properties. The three cases have been applied as detailed in Backman & Paresce (1993), and we have inverted their equations (3), (5), and (6) to solve for D_{BB}, D_{GB}, and D_{ISM} (in units of AU), respectively:

$$D_{\mathrm{BB}} = \left(\frac{278}{T_{\mathrm{dust}}}\right)^2 \left(\frac{L_*}{L_\odot}\right)^{1/2}, \tag{6}$$

$$D_{\mathrm{GB}} = \left(\frac{468}{T_{\mathrm{dust}}}\right)^{5/2} \left(\frac{L_*}{L_\odot}\right)^{1/2} \frac{\lambda_0}{\mu\mathrm{m}} - \frac{1}{2}, \tag{7}$$

$$D_{\mathrm{ISM}} = \left(\frac{636}{T_{\mathrm{dust}}}\right)^{11/4} \left(\frac{L_*}{L_\odot}\right)^{1/2} \left(\frac{T_{\mathrm{eff}}}{T_\odot}\right)^{3/4}. \tag{8}$$

In the relations above T_{dust} is the temperature of the dust grains (corresponding to the temperatures T_{bb} of the excesses in Fig. 1) and $\lambda_0 \sim \langle a \rangle$ is the wavelength shortward of which the radiative efficiency of a grain of size $\langle a \rangle$ is roughly

TABLE 4
Assumed Stellar Parameters

Star	Adopted T_{eff} (K)	R_* ($R_\odot$)	L_* ($L_\odot$)	M_* ($M_\odot$)
HD 145519[a]	11000	2.2	63	2.6
HD 109573A..............	10000	2.0	34	2.4
HD 102647	8500	1.8	15	1.9
HD 107146	6000	1.2	1.7	1.1
HD 88638	5500	1.0	0.88	0.94
HD 17925	5000	1.1	0.37	0.89
CD $-40°8434$[b]	4400	1.39	0.64	...
AA Tau[c].....................	4000	2.1	0.98	0.67
Hen 3-600A[d]..............	3200	2.8	0.72	...

[a] T_{eff} and L_* from de Geus et al. 1989. T_{eff} is rounded to the nearest 500 K for compatibility with Kurucz 1979 models.
[b] Stellar parameters from Gregorio-Hetem & Hetem 2002.
[c] Stellar parameters from Beckwith et al. 1990.
[d] Stellar parameters estimated assuming bolometric correction of -3.24 (for M4 spectral type; Flower 1996) and $V = 12.04$ (Torres et al. 2000).

constant: $\epsilon \sim (1 - \text{albedo}) \sim 1$ (Backman et al. 1997). Note, however, that in fitting the excess in each star, we have only used the blackbody law, without modifications at longer wavelengths where particles of size $a < \lambda$ emit inefficiently. The effect of this is evident in the SEDs of HD 109573A and AA Tau, where at millimeter wavelengths the fitted blackbody overestimates the measured flux.

The inferred dust properties of the detected circumstellar disks are presented in Table 5.

It is important to stress here that, given insufficient constraints from the SED, there exists a degeneracy between the temperature (T_{dust}) and the amount of material (M_{dust}) around a star required to produce a certain fractional excess f_d. This is best seen in the case of HD 17925 in Figure 2. The amount of 250 K debris ($M_{\text{dust}} = 7 \times 10^{-6} \, M_\oplus$, assuming GB particles) required to produce the upper limit on the fractional dust excess in this star ($f_d = 2 \times 10^{-4}$) is *less* than what would be needed ($M_{\text{dust}} = 4 \times 10^{-5} \, M_\oplus$) to produce a smaller excess ($f_d = 6 \times 10^{-5}$) at a cooler temperature (70 K). Yet, the two blackbody temperatures fit the excess in HD 17925 comparatively well ($\chi^2 = 2.3$ and 2.5 per degree of freedom [dof], respectively). The best fit ($\chi^2/\text{dof} = 1.0$) is obtained for a 140 K dust producing a fractional excess $f_d = 7 \times 10^{-5}$, implying $M_{\text{dust}} = 2 \times 10^{-6} \, M_\oplus$.

The same degeneracy is observed in the fit to the SED of HD 88638, as discussed in § 6.1.3. We revisit this observation in § 6.3 when considering the dependence of f_d and M_{dust} on stellar age.

6. DISCUSSION

6.1. Minimum Dust Masses of Stars with Excesses

6.1.1. Known Optically Thick Disks: CD $-40°8434$, AA Tau, and Hen 3-600A

The three coolest stars with disks, CD $-40°8434$, AA Tau, and Hen 3-600A, are young ($\lesssim 10$ Myr), have high disk luminosity fractions ($f_d \sim 0.3$), and likely possess *optically thick* disks. All of them are, in fact, known T Tauri stars. Our estimated disk radii D therefore are not physically meaningful. Detailed modeling of T Tauri disks is beyond the scope of this paper, and we have not therefore attempted to estimate grain sizes and disk masses for these three stars. For in-depth discussion of each case, see Gregorio-Hetem & Hetem (2002; CD $-40°8434$), Chiang et al. (2001; AA Tau; see also Bouvier et al. 1999), and Muzerolle et al. (2000; Hen 3-600A). An estimate of the total disk mass (dust plus gas) exists only for AA Tau (Beckwith et al. 1990; Chiang et al. 2001), and we have listed that in Table 5.

For the remainder of the stars we have assumed that the disks are optically thin, as expected given inferred dust luminosity fractions $f_d \lesssim 0.01$, higher host star temperatures ($T_{\text{eff}} \geq 5000$ K), and older ages ($\gtrsim 10$ Myr).

6.1.2. Known Optically Thin Disks: HD 145519, HD 109573A, HD 102647, and HD 17925

Four stars have already been inferred to harbor debris disks, three of which (HD 109573A, HD 102647, and HD 17925) have been modeled in the previous literature. For these we find that our estimates of the disk parameters are in agreement with the existing ones.

6.1.2.1. HD 145519

HD 145519 (along with HD 147809) has been included in the analysis of Backman et al. (1997) of *ISO* excesses in open cluster A stars. The star possesses only a 60 μm (3.0 σ) excess and, unlike around HD 147809, there are no *IRAS* reject sources or cirrus extractions within a 5′ radius. The *ISO* excess is therefore probably real. The star is not discussed in detail in Backman et al. (1997), and no other measurements of the excess are found in the existing literature.

6.1.2.2. HD 109573A (HR 4796A)

Based solely on the aperture size that we have used for *N*-band photometry (1″ radius for LWS), we can conclude that the detected 10 μm excess in HD 109573A arises within 70 AU of the host star. This is consistent with the extent of the disk predicted by the blackbody and graybody particle assumptions and excludes the possibility for the existence of smaller dust particles with properties similar to those of ISM grains. Our estimate of the size of the debris disk around HD 109573A agrees with previous MIR observations (Jayawardhana et al. 1998; Koerner et al. 1998; Telesco et al. 2000; disk radii 40–70 AU) and with the NICMOS scattered light images of Schneider et al. (1999; disk intensity peaking at 70 AU). The dust mass derived here ($M_{\text{dust}} \gtrsim 0.83 \, M_\oplus = 5.0 \times 10^{27}$ g for GB particles) is consistent with the one derived in Jura et al. (1995; 3×10^{26} g $< M_{\text{dust}} < 8 \times 10^{27}$ g) and with the estimates of Li & Lunine (2003; $M_{\text{dust}} \approx 4.0 – 7.5 \times 10^{27}$ g) found from modeling of the NIR scattered light and of the MIR to submillimeter emission from the HD 109573A disk.

6.1.2.3. HD 102647 (β Leo)

Our disk parameter estimates for HD 102647 ($T_{\text{dust}} = 100 \pm 10$ K, $M_{\text{dust}} \gtrsim 1.7 \times 10^{-3} \, M_\oplus$) agree with those found in the literature. Laureijs et al. (2002a) derive a dust temperature of 83 ± 5 K for HD 102647 from the 25 μm/60 μm *ISO* flux ratio, while Jayawardhana et al. (2001) find $T_{\text{dust}} = 120$ K from blackbody fits to the photosphere and to the IR excess in this star. The amount of dust around HD 102647 inferred from the observations of Laureijs et al. is $1.6 \times 10^{-3} \, M_\oplus$, a number not given in their paper but calculated here based on their assumptions (graybody particles) and their equation (A.5). From submillimeter upper limits, on the other hand, Holmes et al. (2003) find $M_{\text{dust}} < 0.59 M_{\text{Moon}} = 7.3 \times 10^{-3} \, M_\oplus$ ($M_{\text{Moon}} = M_\oplus/81.301$; Heiken, Vaniman, & French 1991). Both results are consistent with the one presented here.

6.1.2.4. HD 17925

Habing et al. (2001) find evidence for a significant *ISO* excess in HD 17925 only at 60 μm (with an upper limit on the flux at 90 μm) and, assuming a disk distance of 50 AU ($T_{\text{eff}} \approx 30$ K) from the star (similar to that in the Vega system), find $M_{\text{dust}} = 1.08 \times 10^{-3} \, M_\oplus$, a value that agrees with our range of estimates. However, by considering the full range of blackbody temperatures consistent with the IR data, we obtain a range of possible masses of the dust disk. Indeed, our measured 1.3 σ *N*-band excess in HD 17925, combined with a 1.3 σ excess at 12 μm ($\Delta[12] = 0.09 \pm 0.07$, from *IRAS*) and a 2.7 σ excess at 25 μm ($\Delta[25] = 0.27 \pm 0.10$ from the averaged *ISO* and *IRAS* flux densities, as adopted by Laureijs et al. 2002a), points to the possible presence of warmer (140 K) material orbiting the star. Recent MIR spectroscopic observations by Gaidos & Koresko (2003) also point to the marginal presence of a silicate emission peak at 7% of the photosphere at 10 μm.

The IR SED of this star can be fitted by a blackbody as warm as $\sim$250 K (Fig. 2), producing an excess of $f_d \approx 3 \times 10^{-4}$. The debris would orbit at a distance of $\sim$7 AU if the particles are graybodies ($\sim$0.8 AU if blackbodies) and would

TABLE 5
DERIVED DISK PROPERTIES

STAR	a_{min} (μm)	$\langle a \rangle$ (μm)	D (AU)			MINIMUM M_{dust}[a] ($M_\oplus$)			t_{PR} (Myr)			MINIMUM M_{PB}[a] ($M_\oplus$)
			BB	GB	ISM	BB	GB	ISM	BB	GB	ISM	
HD 145519	5.7	9.4	700–30	2500–50	10^5–10^3	0.5–0.001	6.5–0.003	4000–0.08	130–0.23	1600–0.6	10^6–10^2	0.009–0.027
HD 109573A.......	3.3	5.5	37	93	1100	0.14	0.83	120	0.38	2.4	340	2.7
HD 102647	1.8	3.1	30	100	840	1.6×10^{-4}	1.7×10^{-3}	0.12	0.32	3.5	250	0.025
HD 107146	0.36	0.60	28	290	890	2.0×10^{-3}	0.22	2.0	0.48	51	480	0.85
HD 88638	0.22	0.36	4–0.03	40–0.08	70–0.09	2×10^{-6} to 6×10^{-8}	2×10^{-4} to 4×10^{-7}	5×10^{-4} to 5×10^{-7}	10^{-2} to 10^{-6}	1 to 10^{-6}	3 to 10^{-5}	0.09–50
HD 17925	0.10	0.16	50–0.8	1000–7	2000–7	5×10^{-6} to 9×10^{-8}	5×10^{-3} to 7×10^{-6}	1×10^{-2} to 7×10^{-6}	2.0–0.0005	2000–0.04	4000–0.04	2×10^{-4} to 2×10^{-2}
CD $-40°8434$.....	...	...	≥ 0.85	≥ 6.9	...	...	...	...	...	...	...	...
AA Tau[b]	...	...	≥ 0.077	≥ 9.1	...	1.8×10^5	1.8×10^5	1.8×10^5	...	...	...	...
Hen 3-600A	...	...	≥ 0.96	≥ 6.3	...	...	...	...	...	...	...	...

[a] The assumed mass of the Earth is $M_\oplus = 5.9736 \times 10^{27}$ g.
[b] Total (dust plus gas) mass from Beckwith et al. 1990; Chiang et al. 2001.
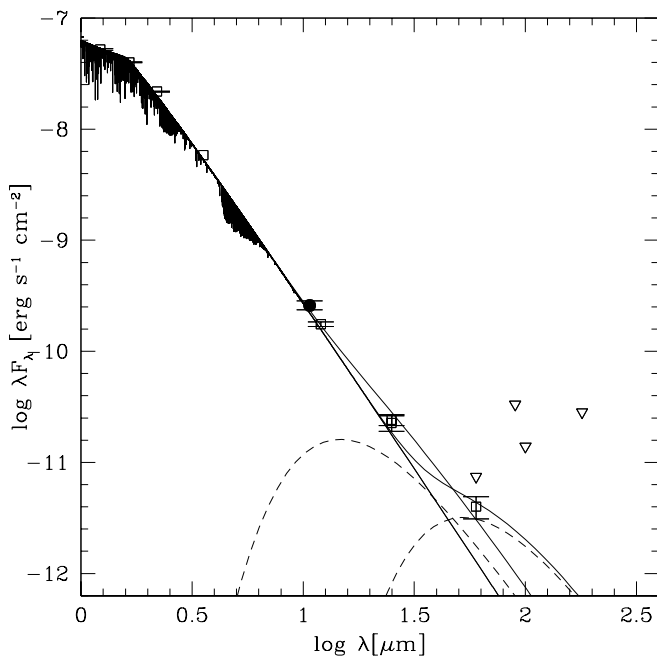
Fig. 2.—Fits to the SED of HD 17925, where 250 and 70 K blackbodies have been allowed to independently account for the excess. Symbols are as in Fig. 1. The NextGen photosphere has been normalized to the J-, H-, and K-band measurements, and the temperature and normalization of the blackbody fit to the excess have been allowed to vary freely. The two cumulative curves (*thick solid lines*) fit the 10–60 μm data comparatively well ($\chi^2/\mathrm{dof} = 2.3$ and 2.5, respectively). However, the hotter (250 K) blackbody produces a higher fractional excess f_d than the cooler (70 K) one by half an order of magnitude, whereas the amount of dust M_{dust} required is less by nearly an order of magnitude. The best fit is achieved with a 140 K blackbody, corresponding to $M_{\mathrm{dust}} \approx 2 \times 10^{-6}$ $M_{\oplus}$. [*See the electronic edition of the Journal for a color version of this figure.*]

have a mass $M_{\mathrm{dust}} \geq 7 \times 10^{-6}$ $M_{\oplus}$ (lower end of the range listed in Table 5), which could make this the least massive debris disk detected outside our solar system. The required mass of parent bodies would be $M_{\mathrm{PB}} \geq 0.015$ $M_{\oplus}$, or $\gtrsim 3$ times the mass of the main asteroid belt in the solar system (Binzel et al. 2000).

Unfortunately, at the level of the 10–25 μm excesses seen in HD 17925 (1–2 σ), we are strongly affected by the accuracy of our assumptions for the model photosphere (mainly the stellar metallicity), as well as by the precision of the JHK photometry for the object, used for the normalization of the model photosphere. Whereas the level of the 10–25 μm excess is 2.0–2.5 σ if the NextGen photosphere is normalized to the J or H apparent magnitude, its significance decreases to 0.3–2.0 σ if the normalization is done at K.

A modest amount of extinction ($A_V \approx 0.2$ mag), a subsolar metallicity ([Fe/H] $\lesssim -1.5$), a subdwarf gravity, or a cooler photosphere (by $\sim$200 K) could all account for the higher MIR fluxes in HD 17925. However, given $f_d \leq 2 \times 10^{-4}$ (Table 3) and the vicinity of the star to the Sun (10 ± 0.1 pc), we expect $A_V < 0.01$. The metal abundance and gravity of the star are very nearly solar (Haywood 2001; Cayrel de Strobel & Cayrel 1989; Perrin 1983), and its temperature is estimated from high-resolution spectroscopy at 5091 K (Cayrel de Strobel & Cayrel 1989; Perrin 1983). None of these factors are thus expected to change the expected stellar SED of HD 17925 between 10 and 25 μm.

Higher precision ($<$0.10 mag) MIR photometry could help constrain the temperature and extent of the debris disk around

HD 17925 but would be difficult to obtain. However, submillimeter imaging can further constrain the SED of the star and could potentially even resolve the emission around it, given its vicinity (10 pc).

6.1.3. *Newly Reported Debris Disks: HD 107146 and HD 88638*

6.1.3.1. HD 107146

From our analysis of the IRAS FSC data on HD 107146, we report a new excess around this star at wavelengths ≥ 60 μm, which is likely due to an orbiting debris disk. Despite a relatively high dust luminosity fraction, $f_d = 1.5 \times 10^{-3}$ (the *IRAS* excesses from known Vega-like stars range from 10^{-3} to 10^{-5}), it has remained overlooked as a result of its apparent faintness. The inferred minimum dust mass M_{dust} (for GB dust particles) is comparable to that in HD 109573A and should be detectable in the submillimeter or in visible scattered light observations (see Williams et al. 2003 for a discussion of a newly observed submillimeter excess in this source). These can then be used to further constrain the spatial extent, morphology, and mass of the debris disk. HD 107146 is one of very few main-sequence G dwarfs known to harbor debris disks (for other candidates in addition to ϵ Eri see Mannings & Barlow 1998; Sylvester & Mannings 2000; Decin et al. 2000). At its intermediate age (50–300 Myr; Table 2) it bridges the gap between the epoch of formation of the solar system and its current evolved state of low dust content.

6.1.3.2. HD 88638

The evidence for a debris disk around HD 88638 is only tentative, expressed as a single 2.4 σ excess at 10.3 μm. The photosphere of the star is below the sensitivity limits of the *IRAS* All-Sky Survey, and it has not been targeted with *ISO*. Longer wavelength, sensitive IR and submillimeter observations (e.g., with *SIRTF*) are needed to confirm the existence of a disk around this star. At the age of HD 88638 ($\sim$600 Myr; Table 2), a debris disk of the inferred mass and distance from the star (Table 5) would bear the closest resemblance to the main asteroid belt in our solar system among all other known stars with debris disks.

In fitting the excess in the SED of HD 88638, we observe the same trend as discussed in the case of HD 17925 (§ 5.2). Because the temperature of the blackbody required to fit the excess is not well constrained, the disk luminosity fraction f_d and the required dust mass M_{dust} are not correlated and are temperature dependent.

6.2. *Dust Mass Limits for Stars Not Detected in Excess*

With the exception of HD 147809, all the stars in our sample that lack an excess are of spectral type G0 and later. The derived upper limits for f_d (assuming 300 K debris disks) indicate $M_{\mathrm{dust}} \lesssim 10^{-5}$ $M_{\oplus}$, assuming that the dust particles behave like graybodies. For comparison, the minimum dust mass detectable around a G0 dwarf in the *ISO* 25 μm survey of Laureijs et al. (2002a) is estimated at 2×10^{-6} $M_{\oplus}$, assuming a 120 K disk. Our survey appears overall slightly less sensitive than theirs, possibly because of our slightly larger median error bars: ± 0.11 mag in ΔN for our ground-based observations versus ± 0.10 mag in $\Delta[25]$ for the *ISO* observations of Laureijs et al. (2002a). However, if we apply the method of dust mass estimation of Laureijs et al. (2002a), we obtain that our N-band observations should be sensitive to disk masses $M_{\mathrm{dust}} \gtrsim 1 \times 10^{-6}$ $M_{\oplus}$ around G0 stars; i.e., our sensitivity is comparable to theirs in terms of the minimum amount of detectable dust mass.

Regardless, from the standpoint of searching for debris disks of different temperatures (and thus radii), the two surveys are complementary.

6.3. *Fractional Excess and Debris Disk Mass versus Stellar Age*

The results of two large studies targeting disk evolution around main-sequence stars with *ISO* and *IRAS* data have shown that the amount of circumstellar dust and the number of stars possessing detectable IR dust excesses are both decreasing functions of stellar age (Spangler et al. 2001; Habing et al. 1999; see also Habing et al. 2001). Given our very limited sample and a bias in the source selection toward stars with known dust disks, we cannot test the conclusions of Habing et al. (1999) and Spangler et al. (2001). We do, however, reproduce the tendency of decreasing dust fraction f_d with age among stars with detected IR excesses (Fig. 3, *top panel*), with a power-law index of -2.0 ± 0.5 ($\chi^2/\mathrm{dof} = 1.6$), compared with -1.76 derived in Spangler et al. (2001). AA Tau and HD 88638 have been excluded from the fit, the dust disk of AA Tau being optically thick (and hence not relevant to the discussion of debris disk evolution) and the excess in HD 88638 being uncertain. Because we are biased toward detecting only the most luminous debris disks, our estimates of f_d delineate only an upper envelope to the actual amount of IR excess present in any object in the 1 Myr–1 Gyr age range.

As discussed in § 5.2, the amount of IR excess f_d is not in a one-to-one correspondence with the mass of emitting circumstellar dust M_{dust}, but it is also a function of the dust temperature or, equivalently, of the distance D of the dust from the star (eq. [3]).

Hotter dust produces larger values of f_d by virtue of a larger area under the Planckian curve, for a fixed dust mass and mean
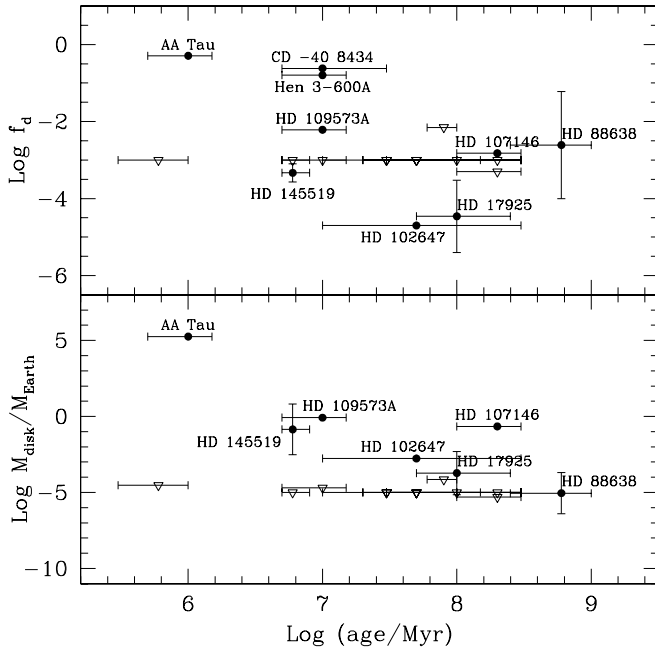
particle size. It would therefore be a coincidence if the f_d-age and M_{dust}-age relations followed the same functional form. This would require that circumstellar dust is maintained at the same temperature around each star, whereas we have examples from our own solar system (zodiacal dust vs. asteroid belt vs. Kuiper Belt) and from other Vega-like systems (e.g., ζ Lep vs. α Lyr vs. ϵ Eri) that dust temperatures range from $\sim$30 to 260 K. One could therefore expect a tighter correlation in the $\log(M_{\mathrm{dust}})$–$\log(\mathrm{age})$ vs. the $\log(f_d)$–$\log(\mathrm{age})$ relation, given that the former is a more physical relationship.

A plot of M_{dust} as a function of stellar age is presented in the bottom panel of Figure 3. The fitted slope is $\log(M_{\mathrm{dust}}) \propto (-3.5 \pm 0.9) \log(\mathrm{age})$ (excluding AA Tau and HD 88638), with a goodness of fit $\chi^2/\mathrm{dof} = 1.7$, similar to the one found for the f_d-age relation above. There is thus no evidence from our limited amount of data that M_{dust} is more tightly correlated with stellar age than f_d. The M_{dust}-age relation is, however, steeper than the one derived by Spangler et al. (2001) and marginally (1.7 σ) inconsistent with that expected for collisionally replenished secondary dust disks (power-law index near -2; Zuckerman & Becklin 1993). The inclusion of the data point due to HD 88638 only strengthens this trend ($\chi^2/\mathrm{dof} = 1.3$ vs. $\chi^2/\mathrm{dof} = 1.7$ for the M_{dust}-age vs. f_d-age case), with the power-law indices remaining approximately unchanged (-3.6 ± 0.7 and -1.7 ± 0.4, respectively), although slightly more discrepant with each other (at the 2.4 σ level, vs. 1.5 σ when HD 88638 is excluded).

Given that M_{dust} is a direct estimate of the dust disk mass and the marginal inconsistency between the two power-law indices, it appears that f_d may be a less adequate tracer of the evolution of dust disks than our estimate of M_{dust}. The

$$M(\text{emitting dust}) \propto f_d \propto \frac{dN}{dt} \propto t_{\mathrm{age}}^{-2} \qquad (9)$$

relation is inferred by Spangler et al. (2001) based on the purely geometric assumption that the collisional rate of large particles dN/dt goes as N^2, where N is the number density of large planetesimals in the system. When the gravitational potentials Gm/a of the planetesimals (where m is the mass of a planetesimal) become comparable to the square of their random velocities v_{rms}^2, the collisional cross sections of the planetesimals increase beyond their simple geometric cross sections because of gravitational focusing. In the two-body approximation, the collision rate is given by (e.g., Safronov 1969)

$$\sigma_g v_{\mathrm{rms}} = \pi a^2 \left(1 + \frac{2Gm}{a v_{\mathrm{rms}}^2}\right) v_{\mathrm{rms}}, \qquad (10)$$

where σ_g is the gravitational cross section. Collisions between planetesimals become more likely with increasing particle size, and their rate goes as a^4, instead of a^2 as in the geometrical regime. The resulting runaway and/or oligarchic growth (Greenberg et al. 1978; Kokubo & Ida 1995) should effectively increase the depletion rate of dust particles faster than $dN/dt \propto t_{\mathrm{age}}^{-2}$; i.e.,

$$M(\text{emitting dust}) \propto \frac{dN}{dt} \propto t_{\mathrm{age}}^{-x}, \qquad (11)$$

where $x > 2$. Hence, the steeper power-law index that we infer ($x \sim -3.5$) presents tentative evidence for planetesimal growth in debris disks.

Fig. 3.—*Top*: f_d vs. stellar age plot. *Bottom*: M_{disk} vs. stellar age plot. In both panels filled circles represent stars with detected IR excesses and are labeled. Downward-pointing open triangles represent upper limits on f_d, or on the dust mass M_{dust}, in systems with no excess IR emission and are not labeled. Vertical error bars are given for HD 17925 and HD 88638, corresponding to the range of inferred dust masses. The error bars on the other points are $\sim$0.5 dex in the top panel and $\sim$1.0 dex in the bottom panel. The data are from Tables 3 and 5, assuming graybody (GB) particle properties.

An important shortcoming of the above discussion is that we do not consider the stars for which we do not find evidence for orbiting debris disks. As noted, as a result of an inherent bias toward stars with known debris disks in our sample, we cannot perform an analysis similar to the ones in Habing et al. (2001) and Spangler et al. (2001). It is significant, however, that a number of our sources do not show any IR excess, when they would be expected to possess such, given universal application of the inferred $\log(M_{\rm dust}) - \log(\rm age)$ relation. The apparent scatter in disk mass versus age may depend on the history of each system and, in particular, on whether favorable conditions for disk retainment had been present throughout the evolution of the star. For instance, the youngest star in our sample, DI Tau, shows no excess emission at 10 μm, a rather atypical state for an M star $\lesssim 1$ Myr old. DI Tau is, however, a binary system with a ~ 20 AU projected separation, and Meyer et al. (1997) argue that the formation of the companion has led to the rapid evolution of the circumstellar disk that may have surrounded DI Tau. On the other hand, HD 145519 (Mathieu, Walter, & Myers 1989) and HD 109573A also reside in binary systems, although they exhibit IR excesses. The separation between the components or conditions other than binarity may be important for the disk dissipation timescale. The spectral type of the star may play a role (Decin et al. 2000), with hotter stars eroding their disks faster, as a result of higher radiation pressures and shorter PR timescales. In addition, the presence or absence of orbiting planets may also affect disk clearing (Goldreich & Ward 1973).

A larger, unbiased sample, including a range of stellar spectral types, as well as single and multiple systems, would be needed to address the issues raised here. More accurate dust mass estimates from disk models, employing realistic grains, would be needed to verify the validity of our suggestion that $M_{\rm dust}$ (as calculated from eq. [3]) is a steeper function of stellar age than f_d and potentially a more adequate tracer of the evolution of debris disks.

7. CONCLUSION

Using ground-based 10 μm observations, we have demonstrated sensitivity to the stellar photosphere of nearby solar-type stars and hence to small excess ($f_d = L_{\rm IR}/L_* \approx 10^{-3}$ for a 300 K debris disk) above it. Our MIR data confirm previous space- and ground-based observations for a subset of our targets and give new insight into this regime for the remainder, by complementing the existing data. By employing simple fitting of the observed IR excesses with blackbody curves, we extract reliable estimates of the ratio f_d of the dust luminosity to the stellar bolometric luminosity. We calculate lower limits on the amount of dust present in each system, after accounting for the effects of radiation pressure and PR drag. Our analysis of the excess in the HD 17925 system points to the fact that it may be the star with the smallest amount of circumstellar dust detected among Vega-like systems to date.

We present strong evidence for the existence of a previously undetected debris disk around HD 107146 and possibly one around HD 88638. Our detection of an excess in HD 107146 from archival *IRAS* FSC data suggests that there may be more stars with unknown debris disks in the deeper and higher signal-to-noise FSC than what is currently known from analyses of the PSC. A methodical search for these in combination with 2MASS NIR photometry, as already presented in Fajardo-Acosta, Beichman, & Cutri (2000) for the PSC, but watchful of the caveats addressed here and the ones described in Song et al. (2002), could therefore prove fruitful. Given that very few disks are found around late-type stars as a result of their intrinsic faintness, the results of such a search could significantly increase the number of known debris disks around solar- and later type stars. Ground-based 10 and 20 μm follow-up observations will be indispensable in discerning *IRAS/ISO* false positives from bona fide MIR excesses, as well as potentially successful in finding new excess candidates (e.g., as in the case of HD 88638).

Based on our limited data, we discuss the possibility of breaking the degeneracy between debris disk temperature and mass in the f_d–stellar age relation. We find that the power-law index in the inferred $M_{\rm dust}$-age relation is steeper than in the f_d-age case and hence tentatively propose the use of the $M_{\rm dust}$-age relation as a better tracer of the evolution of the amount of debris around main-sequence stars. However, a deficiency of the proposed power law is that it does not take into account the absence of debris disks around stars that would be expected to harbor such based on their age. We argue that other factors, such as stellar multiplicity and spectral type, may also play a role.

Future space-based IR observations with *SIRTF* and *SOFIA* are expected to greatly expand the number of known Vega-like stars, by being sensitive to debris disks as faint as the zodiacal dust ($f_d \sim 8 \times 10^{-8}$ Backman & Paresce 1993) around nearby stars as evolved as our Sun. These will provide the database necessary to answer the prominent questions about the processes and timescales of evolution of debris disks around main-sequence stars and will place our own solar system in the context of stellar and planetary evolution.

REFERENCES

Allen, C. W. 1973, Astrophysical Quantities (London: Athlone)
Allende Prieto, C., & Lambert, D. L. 1999, A&A, 352, 555
Artymowicz, P. 1988, ApJ, 335, L79
Aumann, H. H., & Probst, R. G. 1991, ApJ, 368, 264
Aumann, H. H., et al. 1984, ApJ, 278, L23
Backman, D. E., Fajardo-Acosta, S. B., Stencel, R. E., & Stauffer, J. R. 1997, Ap&SS, 255, 91
Backman, D. E., & Paresce, F. 1993, in Protostars and Planets III, ed. E. H. Levy & J. I. Lunine (Tucson: Univ. Arizona Press), 1023–1304

Barrado y Navascuès, D. 1998, A&A, 339, 831
Beckwith, S. V. W., Sargent, A. I., Chini, R. S., & Güsten, R. 1990, AJ, 99, 924
Beichman, C. A., Neugebauer, G., Habing, H. J., Clegg, P. E., & Chester, T. J. 1988 (eds.), *Infrared Astronomical Satellite* Catalogs and Atlases, Vol. 1, Explanatory Supplement (NASA RP-1190; Washington, DC: GPO)
Binzel, R. P., Hanner, M. A., & Steel, D. I. 2000, in Allen's Astrophysical Quantities, ed. A. N. Cox (New York: Springer), 315
Bouvier, J., et al. 1999, A&A, 349, 619

Burns, J. A., Lamy, P. L., & Soter, S. 1979, Icarus, 40, 1
Cayrel de Strobel, G., & Cayrel, R. 1989, A&A, 218, L9
Chen, C. H., & Jura, M. 2001, ApJ, 560, L171
Chiang, E. I., Joung, M. K., Creech-Eakman, M. J., Qi, C., Kessler, J. E., Blake, G. A., & van Dishoeck, E. F. 2001, ApJ, 547, 1077
Cohen, M., Walker, R. G., Barlow, M. J., & Deacon, J. R. 1992, AJ, 104, 2045
Cohen, M., Wheaton, W. A., & Megeath, S. T. 2003, AJ, 126, 1090
Cutri, R. M., et al. 2003, Explanatory Supplement to the 2MASS All Sky Data Release
Decin, G., Dominik, C., Malfait, K., Mayor, M., & Waelkens, C. 2000, A&A, 357, 533
de Geus, E. J., de Zeeuw, P. T., & Lub, J. 1989, A&A, 216, 44
de Jager, C., & Nieuwenhuijzen, H. 1987, A&A, 177, 217
Drilling, J. S., & Landolt, A. U. 2000, in Allen's Astrophysical Quantities, ed. A. N. Cox (New York: Springer), 389
Eggen, O. 1998, AJ, 116, 1810
Fajardo-Acosta, S. B., Beichman, C. A., & Cutri, R. M. 2000, ApJ, 538, L155
Fajardo-Acosta, S. B., Stencel, R. E., Backman, D. E., & Thakur, N. 1999, ApJ, 520, 215
Flower, P. J. 1996, ApJ, 469, 355
Gaidos, E., & Koresko, C. 2003, NewA, 9, 33
Goldreich, P., & Ward, W. R. 1973, ApJ, 183, 1051
Greaves, J. S., et al. 1998, ApJ, 506, L133
Greenberg, R., & Nolan, M. C. 1989, in Asteroids II, ed. R. P. Binzel, T. Gehrels, & M. S. Matthews (Tucson: Univ. Arizona Press), 778
Greenberg, R., Wacker, J., Chapman, C. R., & Hartman, W. K. 1978, Icarus, 35, 1
Gregorio-Hetem, J., & Hetem, A., Jr. 2002, MNRAS, 336, 197
Gregorio-Hetem, J., Lépine, J. R. D., Quast, G. R., Torres, C. A. O., & de la Reza, R. 1992, AJ, 103, 549
Habing, H. J., et al. 1999, Nature, 401, 456
———. 2001, A&A, 365, 545
Hauschildt, P. H., Allard, F., & Baron, E. 1999, ApJ, 512, 377
Hayward, T. L., Houck, J. R., & Miles, J. W. 1996, SpectroCam-10 User's Manual
Hayward, T. L., Miles, J. E., Houck, J. R., Gull, G. E., & Schoenwald, J. 1993, Proc. SPIE, 1946, 334
Haywood, M. 2001, MNRAS, 325, 1365
Heiken, G., Vaniman, D., & French, B. M. 1991, in Allen's Astrophysical Quantities, ed. A. N. Cox (New York: Springer), 309
Holland, W. S., et al. 1998, Nature, 392, 788
Hollenbach, D. J., Yorke, H. W., & Johnstone, D. 2000, in Protostars and Planets IV, ed. V. Mannings, A. P. Boss, & S. S. Russell (Tucson: Univ. Arizona Press), 401
Holmes, E. K., Butner, H. M., Fajardo-Acosta, S. B., & Rebull, L. M. 2003, AJ, 125, 3334
Houck, N., & Swift, C. 1999, Michigan Catalogue of Two-dimensional Spectral Types for the HD stars, Vol. 5 (Ann Arbor: Univ. Michigan)
Jayawardhana, R., Fisher, R. S., Hartmann, L., Telesco, C., Piña, R., & Fazio, G. 1998, ApJ, 503, L79
Jayawardhana, R., Fisher, R. S., Telesco, C. M., Piña, R. K., Barrado y Navascuès, D., Hartmann, L. W., & Fazio, G. G. 2001, AJ, 122, 2047
Jayawardhana, R., Hartmann, L., Fazio, G., Fisher, R. S., Telesco, C. M., & Piña, R. K. 1999a, ApJ, 520, L41
———. 1999b, ApJ, 521, L129
Jeffries, R. D. 1995, MNRAS, 273, 559
Jones, B., & Puetter, R. C. 1993, Proc. SPIE, 1946, 610
Jones, D. H. P. 1971, MNRAS, 152, 231
Jura, M. 1991, ApJ, 383, L79
Jura, M., Ghez, A. M., White, R. J., McCarthy, D. W., Smith, R. C., & Martin, P. G. 1995, ApJ, 445, 451
Jura, M., Malkan, M., White, R. J., Telesco, C., Piña, R., & Fisher, R. S. 1998, ApJ, 505, 897
Jura, M., Zuckerman, B., Becklin, E. E., & Smith, R. C. 1993, ApJ, 418, L37
Kenyon, S. J., & Hartmann, L. 1995, ApJS, 101, 117
Koerner, D. W., Ressler, M. E., Werner, M. W., & Backman, D. E. 1998, ApJ, 503, L83

Kokubo, E., & Ida, S. 1995, Icarus, 114, 247
Krelowski, J., & Strobel, A. 1983, A&A, 127, 271
Kurucz, R. L. 1979, ApJS, 40, 1
———. 1992, Rev. Mexicana Astron. Astrofis., 23, 181
Laureijs, R. J., Jourdain de Muizon, M., Leech, K., Siebenmorgen, R., Dominik, C., Habing, H. J., Trams, N., & Kessler, M. F. 2002a, A&A, 387, 285
Laureijs, R. J., Klaas, U., Richards, P. J., Schulz, B., & Ábrahaám, P. 2002b, The ISO Handbook, Vol. 4
Leggett, S. K., et al. 2002, ApJ, 564, 452
Li, A., & Lunine, J. I. 2003, ApJ, 590, 368
Lisse, C., et al. 2002, ApJ, 570, 779
Mannings, V., & Barlow, M. J. 1998, ApJ, 497, 330
Mathieu, R. D. Walter, F. M., & Myers, P. C. 1989, AJ, 98, 987
Mathis, J. S. 1990, ARA&A, 28, 37
Meyer, M. R., Beckwith, S. V. W., Herbst, T. M., & Robberto, M. 1997, ApJ, 489, L173
Meyer, M. R., Wilking, B. A., & Zinnecker, H. 1993, AJ, 105, 619
Montes, D., Lòpez-Santiago, J., Gàlvez, M. C., Fernàndez-Figueroa, M. J., De Castro, E., & Cornide, M. 2001, MNRAS, 328, 45
Moshir, M., et al. 1992, Explanatory Supplement to the IRAS Faint Source Survey, Version 2 (JPL D-10015 8/92; Pasadena: JPL)
Muzerolle, J., Calvet, N., Briceño, C., Hartmann, L., & Hillenbrand, L. 2000, ApJ, 535, L47
Nakagawa, Y., Hayashi, C., & Nakazawa, K. 1983, Icarus, 54, 361
O'Dell, M. A., Hendry, M. A., & Collier Cameron, A. 1994, MNRAS, 268, 181
Perrin, M.-N. 1983, A&A, 128, 347
Randich, S., Martin, E. L., Garcia Lopez, R. J., & Pallavivini, R. 1998, A&A, 333, 591
Rieke, G. H., Lebofsky, M. J., & Low, F. J. 1985, AJ, 90, 900
Ryter, C., Puget, J. L., & Pèrault, M. 1987, A&A, 186, 312
Safronov, V. S. 1969, in Evolution of the Protoplanetary Cloud and Formation of the Earth and the Planets (Jerusalem: Israel Program for Scientific Translations), 63
Schneider, G., et al. 1999, ApJ, 513, L127
Silverstone, M. D. 2000, Ph.D. thesis, UCLA
Skrutskie, M. E., et al. 1990, AJ, 99, 1187
Song, I., Caillault, J.-P., Barrado y Navascuès, D., & Stauffer, J. 2001, ApJ, 546, 352
Song, I., Weinberger, A., Becklin, E. E., Zuckerman, B., & Chen, C. 2002, AJ, 124, 514
Spangler, C., Sargent, A. I., Silverstone, M. D., Becklin, E. E., & Zuckerman, B. 2001, ApJ, 555, 932
Stassun, K. G., Mathieu, R. D., Vrba, F. J., Mazeh, T., & Henden, A. 2001, AJ, 121, 1003
Stencel, R. E., & Backman, D. E. 1991, ApJS, 75, 905
Sterzik, M. F., Alcalá, J. M., Covino, E., & Petr, M. G. 1999, A&A, 346, L41
Stetson, P. B. 1987, PASP, 99, 191
Strassmeier, K. G., Washuettl, A. Granzer, T., Scheck, M., & Weber, M. 2000, A&AS, 142, 275
Strom, K. M., Strom, S. E., Edwards, S., Cabrit, S., & Skrutskie, M. F. 1989, AJ, 97, 1451
Sylvester, R. J., & Mannings, V. 2000, MNRAS, 313, 73
Telesco, C. M., et al. 2000, ApJ, 530, 329
Tokunaga, A. T. 1984, AJ, 89, 172
Torres, C. A. O., da Silva, L., Quast, G. R., de la Reza, R., & Jilinski, E. 2000, AJ, 120, 1410
Waters, L. B. F. M., Cotè, J., & Aumann, H. H. 1987, A&A, 172, 225
Webb, R. A., Zuckerman, B., Platais, I., Patience, J., White, R. J., Schwartz, M. J., & McCarthy, C. 1999, ApJ, 512, L63
Weinberger, A. J., et al. 2002, ApJ, 566, 409
Wichmann, R., Schmitt, J. H. M. M., & Hubrig, S. 2003, A&A, 399, 983
Williams, J. P., Najita, J., Liu, M. C., Bottinelli, S., Carpenter, J. M., Hillenbrand, L. A., Meyer, M. R., & Soderblom, D. 2003, ApJ, submitted
Wilner, D. J., Holman, M. J., Kuchner, M. J., & Ho, P. T. P. 2002, ApJ, 569, L115
Zuckerman, B., & Becklin, E. E. 1993, ApJ, 414, 793

Note added in proof.—It has been brought to our attention that HD 107146 has been previously identified as a Vega-like star from *IRAS* in the Ph.D. thesis work of M. D. Silverstone (2000, UCLA). His estimate of the MIR excess in this star (10^{-3}) agrees with ours (1.5×10^{-3}).